

1 **Fast Evolution of SOS-Independent Multi-Drug Resistance in Bacteria**

2

3 Le Zhang^{1,†}, Yunpeng Guan^{1†}, Yuen Yee Cheng¹, Nural N. Cokcetin², Amy L. Bottomley²,
4 Andrew Robinson³, Elizabeth J. Harry², Antoine van Oijen³, Qian Peter Su^{1#}, Dayong Jin^{1#}

5

6 ¹Institute for Biomedical Materials and Devices (IBMD), University of Technology Sydney,
7 Ultimo, Australia.

8 ²Australian Institute for Microbiology & Infection (AIMI), University of Technology Sydney,
9 Ultimo, Australia.

10 ³School of Chemistry and Molecular Bioscience, University of Wollongong, Wollongong,
11 Australia.

12 †These authors contributed equally to this work

13 #Corresponding author. Email: qian.su@uts.edu.au; dayong.jin@uts.edu.au

14

15 **Abstract**

16 The killing mechanism of many antibiotics involves the induction of DNA damage, either
17 directly or indirectly, which activates the SOS response. RecA, the master regulator of the
18 SOS response, has shown to play a central role in the evolution of resistance to
19 fluoroquinolones, even after short-term exposure. While this paradigm is well established for
20 DNA-damaging antibiotics, it remains unclear whether β -lactams elicit similar resistance
21 dynamics or depend on RecA and SOS-mediated mechanisms. In this study, we observed a
22 rapid and stable evolution of β -lactam resistance (20-fold MIC increase within 8 hours) in
23 *Escherichia coli* lacking RecA after a single exposure to ampicillin. Contrary to expectation,
24 this resistance emerged through an SOS-independent mechanism involving two distinct
25 evolutionary forces: increased mutational supply and antibiotic-driven selection. Specifically,
26 we found that RecA deletion impaired DNA repair and downregulated base excision repair
27 pathways, while concurrently repressing the transcription of antioxidative defence genes.
28 This dual impairment led to excessive accumulation of reactive oxygen species (ROS), which
29 in turn promoted the emergence of resistance-conferring mutations. While ampicillin
30 treatment did not alter survival, it selectively enriched for rare mutants arising in the RecA-
31 deficient and ROS-elevated background. Collectively, our findings demonstrate that this
32 oxidative environment, together with compromised DNA repair capacity, increases genetic
33 instability and creates a selective landscape favouring the expansion of resistant

34 clones. These results highlight the repair-redox axis as a key determinant of bacterial
35 evolvability under antimicrobial stress.

36

37 **Introduction**

38 Addressing bacterial infections caused by emerging and drug-resistant pathogens represents a
39 major global health priority. Bactericidal antibiotics can exert their effects on cells by directly
40 or indirectly causing DNA damage or triggering the production of highly destructive
41 hydroxyl radicals (1-3). This, in turn, initiates a protective mechanism known as the SOS
42 response, which enables bacterial survival against the lethal impacts of antibiotics by
43 activating intrinsic pathways for DNA repair (4-7). The activation of DNA repair processes
44 relies on specific genes, such as *recA*, which encodes a recombinase involved in DNA repair,
45 and *lexA*, a repressor of the SOS response that can be inactivated by RecA (8).

46

47 Studies have demonstrated that a single exposure to fluoroquinolones, a type of antibiotic that
48 induces DNA breaks and triggers the SOS response, leads to the development of bacterial
49 resistance in *Escherichia coli* (*E. coli*) through a RecA and SOS response-dependent
50 mechanism (9). Given the crucial role of RecA in the SOS response, inhibiting RecA activity
51 to deactivate the SOS response presents an appealing strategy for preventing the evolution of
52 bacterial resistance to antibiotics (10). Similarly, exposure to fluoroquinolones induces the
53 SOS response and mutagenesis in *Pseudomonas aeruginosa*, and the deletion of *recA* in this
54 pathogen results in a significant reduction in resistance to fluoroquinolones (11).

55

56 Unlike fluoroquinolones, β -lactam antibiotics induce a RecA-dependent SOS response in *E.*
57 *coli* through impaired cell wall synthesis, mediated by the DpiBA two-component signal
58 system (12). The development of antibiotic resistance, triggered by exposure to β -lactams,
59 has been extensively investigated using the cyclic adaptive laboratory evolution (ALE)
60 method. Mutations that arise during cyclic ALE experiments are attributed to errors occurring
61 during continued growth, necessitating multiple rounds of β -lactam exposure to drive the
62 evolution of resistance in *E. coli* cells (13,14). However, the precise roles of RecA and SOS
63 responses in the development of resistance under short-term β -lactam antibiotics exposure
64 remain unclear.

65

66 Recently, there has been a growing interest in understanding the impact of the stress-induced
67 accumulation of reactive oxygen species (ROS) on bacterial cells (15,16). While exploring

68 methods to harness ROS-mediated killing has the potential to enhance the effectiveness of
69 various antibiotics (17-19), the role of ROS in antimicrobial activity has become a topic of
70 controversy following challenges to the initial observations (20,21). The generation of ROS
71 has been found to contribute to the development of multidrug resistance, as prolonged
72 exposure to antibiotics in cyclic ALE experiments is known to generate ROS, leading to
73 DNA damage and increased mutagenesis (22,23). Nevertheless, there is still limited
74 knowledge regarding the consequences of ROS accumulation in bacteria when the activity of
75 RecA or the SOS response is suppressed.

76

77 Here, we report that a single exposure to β -lactam antibiotics can rapidly drive the evolution
78 of multidrug resistance in *E. coli* lacking RecA. This process reflects a two-step evolutionary
79 mechanism: RecA deficiency increases mutational supply by impairing DNA repair,
80 repressing antioxidant gene expression, and promoting ROS accumulation; subsequently,
81 antibiotic pressure selectively enriches resistant variants from this hypermutable population.

82

83 **Results**

84 **Single β -lactam exposure accelerates resistance evolution in the *recA* mutant strain 85 through a selection-driven mechanism**

86 To investigate the impact of the SOS response on bacterial evolution towards β -lactam
87 resistance, we generated a *recA* mutant strain ($\Delta recA$) from the *E. coli* MG1655 strain.
88 Initially, we conducted an ALE experiment using a slightly modified treatment protocol (24)
89 on the wild type and $\Delta recA$ strains. During a period of three weeks, the cells were subjected
90 to cycles of ampicillin exposure for 4.5 hours at a concentration of 50 μ g/mL (10 times the
91 MIC) each day (Figure 1-figure supplement 1A) (25). As anticipated based on previous
92 studies, the intermittent ampicillin treatments over the course of three weeks resulted in the
93 evolution of antibiotic resistance in the wild type strain (Figure 1-figure supplement 1B).
94 However, a significantly accelerated development of resistance was found in the $\Delta recA$ strain,
95 with the average time to resistance reduced to 2 days (Figure 1-figure supplement 1B). More
96 importantly, we observed that resistance even emerged in the $\Delta recA$ strain after a single
97 exposure for 8 hours to ampicillin (Fig. 1A-C). Meanwhile, after 8 hours of treatment with 50
98 μ g/mL ampicillin, the survival rates of both wild type and $\Delta recA$ strain were consistent
99 (Figure 1-figure supplement 2). To ensure that the emergence of resistance we observed was
100 not illusory due to technical issues during the *recA* knockout process, we employed another
101 $\Delta recA$ strain (JW2669-1) provided by the Coli Genetic Stock Centre (CGSC) with the same

102 killing procedure. The results from both bacterial strains were consistent (Figure 1-figure
103 supplement 3A and B). To further investigate, we treated both the wild type and $\Delta recA$ cells
104 with other β -lactams, including penicillin G and carbenicillin, at concentrations equivalent to
105 10 times the MIC (1 mg/mL and 200 μ g/mL, respectively) for 8 hours (26,27). Consistently,
106 these treatments also led to a fast evolution of antibiotic resistance in the $\Delta recA$ strain (Figure
107 1-figure supplement 4A and B).

108

109 To assess the stability of this accelerated antibiotic resistance acquired by the $\Delta recA$ strain,
110 we conducted a study wherein the $\Delta recA$ resistant isolates, originating from the initial 8-hour
111 treatment with ampicillin, were continuously cultivated in a medium devoid of antibiotics for
112 a period of seven days. Our findings revealed that once resistance was established, resistance
113 remained stable and was able to be passed on to subsequent generations even in the absence
114 of ampicillin (Fig. 1D). Moreover, we performed a complementation experiment by
115 introducing a plasmid containing *recA* under its native promoter into the $\Delta recA$ strain prior to
116 Step i in Fig. 1A, that is, before exposing the cells to ampicillin. Interestingly, this
117 complemented strain displayed a comparable MIC to the isogenic wild type strain and
118 maintained its sensitivity even after ampicillin treatment for up to 8 hours (Fig. 1E).

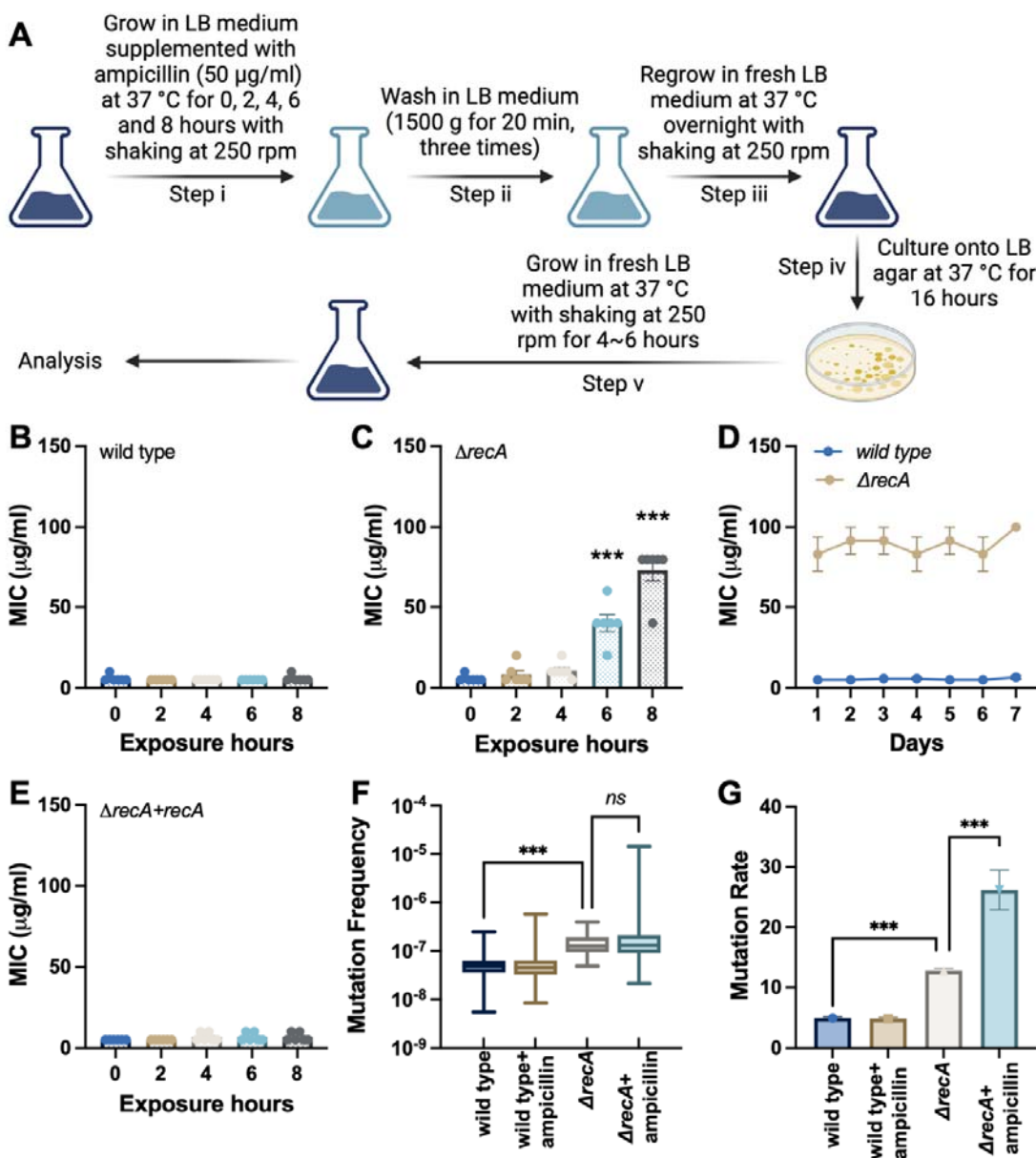
119

120 Antibiotic resistance evolves through the combined effects of mutational events and selection
121 imposed by antimicrobial pressure (28). To clarify which mechanism underlies the rapid
122 emergence of resistance in the $\Delta recA$ strain, we systematically analysed the mutation
123 frequency and distribution patterns in response to ampicillin treatment. Fig. 1F shows the
124 distribution of rifampicin-resistant colony-forming units (CFUs) across 96 independent
125 cultures of the wild type and $\Delta recA$ strains, with and without exposure to ampicillin (50
126 μ g/mL for 8 hours). Although the treatment of ampicillin in the $\Delta recA$ strain displayed a
127 highly skewed distribution with apparent jackpot cultures, non-parametric statistical
128 comparison (Kruskal-Wallis with Dunn's test) did not detect a significant difference in
129 overall mutation frequency compared to untreated $\Delta recA$. This suggests that while the median
130 mutation burden remained stable, rare resistant outliers were significantly enriched, which
131 was a pattern consistent with selection rather than broad mutagenesis (29). Further, using the
132 maximum likelihood estimation (MLE) (30), we calculated the mutation rates (mutations per
133 culture) for each group (Fig. 1G). While the $\Delta recA$ group exhibited a modest increase in
134 baseline mutation rate compared to the wild type strain, the addition of ampicillin led to a
135 significant increase in estimated mutation rate.

136

137 To further assess the statistical properties of these distributions, we fitted the observed data to
138 a Poisson model (Figure 1-figure supplement 5A). The mutation frequency distributions in
139 the wild type strain with or without the treatment of ampicillin conformed well to Poisson
140 expectations, consistent with random spontaneous mutation events. In contrast, the single
141 exposure to ampicillin significantly deviated from the Poisson model, indicating a non-
142 random clonal enrichment process in the $\Delta recA$ strain (31). Finally, we applied a fluctuation
143 test-based inference framework grounded in the Luria-Delbrück model to distinguish between
144 mutation induction and clonal selection (32). As shown in Figure 1-figure supplement 5B,
145 only the $\Delta recA$ strain treated with ampicillin exhibited a markedly non-Poisson distribution of
146 mutant counts, characterized by a long right-skewed tail and the emergence of jackpot
147 cultures. This distribution is inconsistent with uniform mutagenesis and instead supports a
148 model in which antibiotic treatment selectively enriches rare early-arising resistant
149 subpopulations. Together, these findings demonstrate that a single exposure to β -lactam
150 antibiotics promotes a rapid and heritable evolution of antibiotic resistance in the $\Delta recA$ strain,
151 predominantly through selection rather than *de novo* induction of mutations.

152



153

154 **Figure 1. Fast evolution of antibiotic resistance in *E. coli* recA mutant strain. (A)**
155 Experimental flow for the single exposures to antibiotics in *E. coli* strains. Step i: an
156 overnight culture (1×10^9 CFU/mL cells) was diluted 1:50 into 30 mL LB medium
157 supplemented with 50 μ g/mL ampicillin and incubated at 37°C with shaking at 250 rpm for 0,
158 2, 4, 6 and 8 hours; Step ii: after each treatment, the ampicillin containing medium was
159 removed by washing twice in a fresh LB medium; Step iii: the surviving isolates were
160 resuspended in 30 mL fresh LB medium and regrown overnight at 37°C with shaking at 250
161 rpm; Step iv: cell cultures were plated onto LB agar and incubated for 16 hours at 37°C; Step
162 v: single colonies were inoculated in 30 mL fresh LB medium and cultured at 37°C with
163 shaking at 250 rpm for 4 to 6 hours. (B) MICs of ampicillin were measured against the wild

164 type *E. coli* strain after single exposures to ampicillin. **(C)** MICs of ampicillin were measured
165 against the $\Delta recA$ strain after single exposures to ampicillin. **(D)** After the treatment of Step v,
166 cells were continuously cultured in an antibiotic-free medium for seven days. MICs of
167 ampicillin were measured each day. **(E)** MICs of ampicillin were measured against the $\Delta recA$
168 strain treated with ampicillin, where the expression of RecA was restored using plasmid-
169 based constitutive expression of *recA* before the treatment of Step i. **(F)** Distribution of
170 rifampicin-resistant mutant counts following single β -lactam exposure (96 replicate cultures
171 in each group). Statistical comparison of mutation frequency (median values) used the
172 Kruskal-Wallis test followed by Dunn's multiple comparisons. **(G)** Mutation rate (mutations
173 per culture) estimates derived by maximum likelihood analysis. Each experiment was
174 independently repeated at least six times using parallel replicates, and the data are shown as
175 mean \pm SEM. Significant differences among different treatment groups are analysed by
176 independent t-test, * $P < 0.05$, ** $P < 0.01$, *** $P < 0.001$, ns, no significance.

177

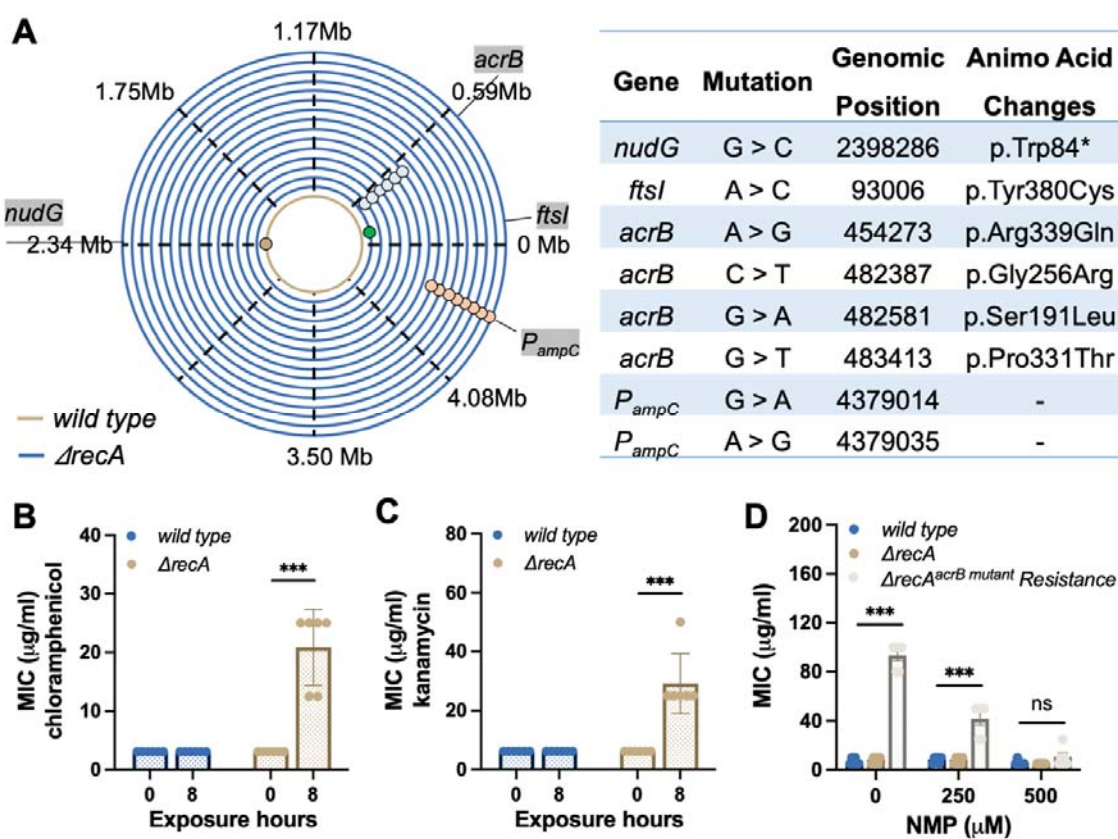
178 **Detection of drug resistance associated DNA mutations in *recA* mutant resistant isolates**

179 In bacteria, resistance to most antibiotics requires the accumulation of drug resistance
180 associated DNA mutations that can arise stochastically and, under stress conditions, become
181 enriched through selection over time to confer high levels of resistance (33). Having observed
182 a non-random and right-skewed distribution of mutation frequencies in $\Delta recA$ isolates
183 following ampicillin exposure, we next sought to determine whether specific resistance-
184 conferring mutations were enriched in $\Delta recA$ isolates following antibiotic exposure. We
185 thereby randomly selected 15 colonies on non-selected LB agar plates from the wild type
186 surviving isolates, and antibiotic screening plates containing 50 μ g/mL ampicillin from the
187 $\Delta recA$ resistant isolates, respectively, and performed whole-genome sequencing. We found
188 that drug resistance associated mutations were present in all resistant isolates, including the
189 mutations in the promoter of the β -lactamase *ampC* (P_{ampC}) in 8 isolates, the ampicillin-
190 binding target PBP3 (*ftsI*) in 1 isolate, and the AcrAB-TolC subunit AcrB (*acrB*) mutations in
191 6 isolates (Fig. 2A). A mutation in gene *nudG* was detected in wild type surviving isolates
192 after the single exposure to ampicillin (Fig. 2A), which is involved in pyrimidine (d)NTP
193 hydrolysis to avoid DNA damage (34). Other mutations were listed in the Table S1.

194

195 The presence of P_{ampC} mutations was accompanied by a significant increase in the production
196 of β -lactamase in bacteria (Figure 2-figure supplement 1). This leads to specific resistance to

197 β -lactam antibiotics. The gene *acrB* codes for a sub-component of the AcrAB-TolC multi-
198 drug efflux pump, which is central in Gram-negative bacteria (35,36). Mutations in AcrAB-
199 TolC enhance the efflux of antibiotics and confer resistance to multiple drugs (35).
200 Consequently, after short-term exposure to ampicillin, the $\Delta recA$ isolates carrying the *acrB*
201 mutations exhibited resistance to other types of antibiotics, such as chloramphenicol and
202 kanamycin (Fig. 2B and C). Treatment with high concentrations of 1-(1-Naphthylmethyl)
203 piperazine (NMP), an efflux pump inhibitor (EPI) that competitively blocks TolC-composed
204 efflux pumps, successfully restored the sensitivity of $\Delta recA$ resistant isolates to ampicillin,
205 bringing them back to the equivalent concentrations found in the wild type (Fig. 2D).
206 Collectively, these results suggest that β -lactam treatment rapidly selects for resistance-
207 conferring mutations, which were enriched in $\Delta recA$ isolates following short-term exposure.
208



210 **Figure 2. Rapid induction of drug resistance associated DNA mutations in the *recA*
211 mutant strain. (A)** Detection of drug resistance associated DNA mutations in the wild type
212 and $\Delta recA$ strain after the single exposures to ampicillin at 50 μ g/mL for 8 hours. **(B)** MICs
213 of chloramphenicol against the wild type and $\Delta recA$ strain after the single treatment with
214 ampicillin were tested. **(C)** MICs of kanamycin against the wild type and $\Delta recA$ strain after

215 the single treatment with ampicillin were tested. **(D)** The wild type, *ΔrecA*, and *ΔrecA^{acrB}*
216 *mutant* resistant isolates were incubated with NMP at different concentrations for 12 hours.
217 Subsequently, MICs were tested in these strains for resistance to ampicillin. Each experiment
218 was independently repeated at least six times, and the data is shown as mean \pm SEM.
219 Significant differences among different treatment groups are analyzed by independent t-test,
220 $*P < 0.05$, $**P < 0.01$, $***P < 0.001$, *ns*, no significance.
221

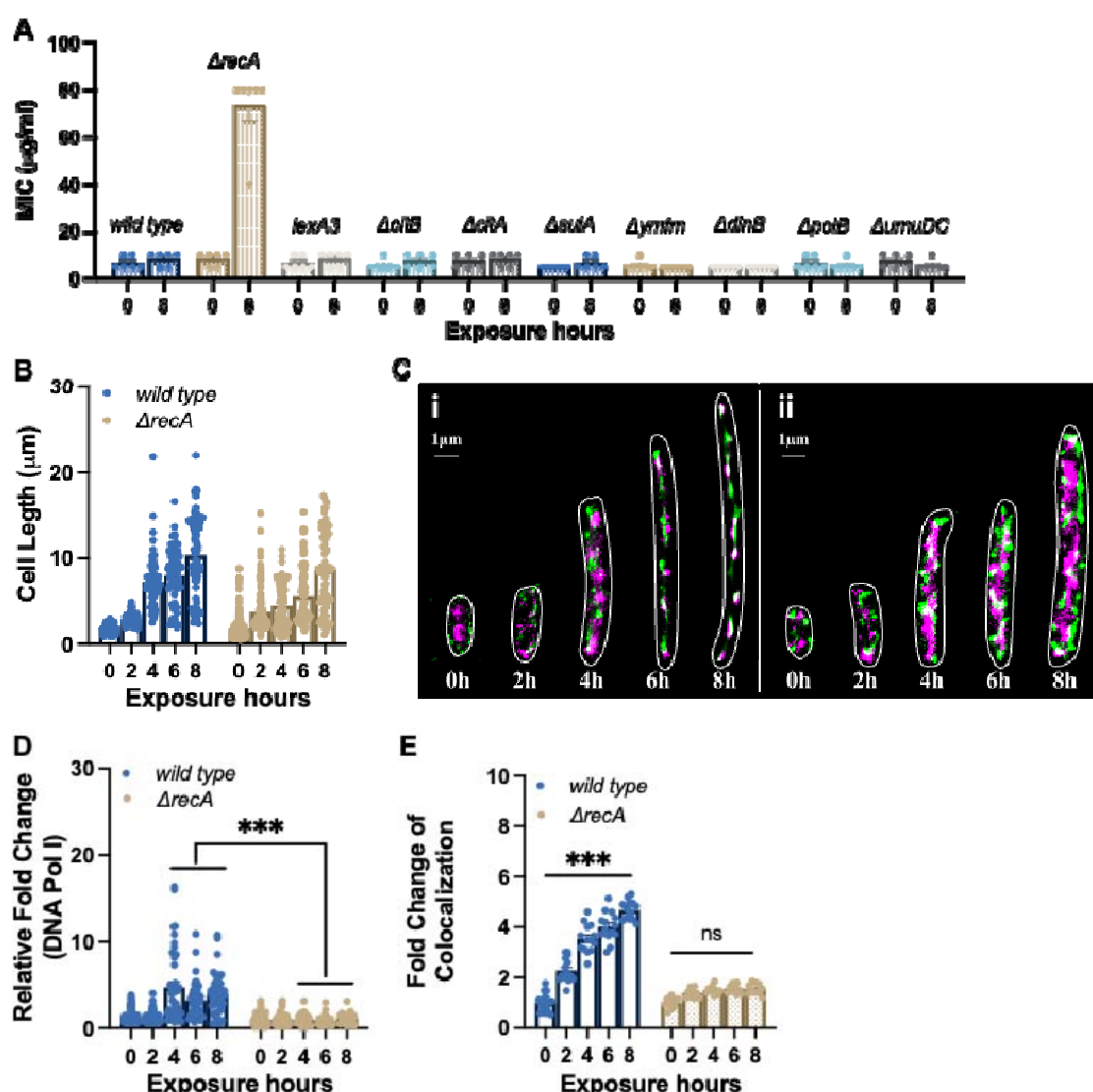
222 **Hindrance of SOS-independent DNA repair in *recA* mutant resistant isolates**

223 Impairment of DNA damage repair can accelerate the accumulation of mutations and
224 influence bacterial adaptability under antibiotic stress. While RecA is best known for
225 regulating the SOS response, we asked whether its absence also impacts resistance evolution
226 through SOS-dependent or -independent repair mechanisms. To investigate it, we first tested
227 the ability of various mutants involved in different pathways of the SOS response to evolving
228 antibiotic resistance following a single treatment with ampicillin for 8 hours at 50 μ g/mL. A
229 mutant form of the SOS master regulator LexA (*lexA3*), which is incapable of being cleaved
230 and thus defective in SOS induction, did not exhibit antibiotic resistance evolution (Fig. 3A).
231 Additionally, the deletion of either DpiB or DpiA (encoded by *citB* or *citA*, respectively),
232 inhibiting the DpiBA two-component signal transduction system, did not result in the
233 development of antibiotic resistance after ampicillin exposure (Fig. 3A). Moreover, the
234 deletion of several downstream effectors of the SOS response, including those involved in
235 cell division inhibition (SulA and YmfM encoded by *sulA* and *ymfM*) (37) (Fig. 3A), and
236 DNA repair (DNA Pol II, DNA Pol IV, and DNA Pol V encoded by *polB*, *dinB* and *umuDC*)
237 (38) also did not lead to the evolution of antibiotic resistance (Fig. 3A). These results indicate
238 that the rapid resistance evolution observed in the *ΔrecA* strain is not mediated by SOS
239 pathway mutants, suggesting that RecA governs resistance evolution through SOS-
240 independent mechanisms.
241

242 In addition to the DNA repair components associated with the SOS response, DNA Pol I
243 plays a role in processing RNA primers during lagging-strand synthesis and filling small gaps
244 during DNA repair reactions (39). Since DNA Pol I (encoded by *polA*) has been
245 demonstrated as an essential gene required for the growth of *E. coli* in rich medium,
246 including the LB medium (40,41), we next utilized Single Molecule Localization Microscopy
247 (SMLM) to precisely locate the chromosome and DNA Pol I in a dynamic manner. During an

248 8 hour exposure to ampicillin, we observed the formation of multinucleated filaments in both
249 the wild type and $\Delta recA$ strain, indicating a pause in cell division and suggesting a time
250 period for bacterial DNA repair to take place (Fig. 3B and C) (42). However, the expression
251 level of DNA Pol I was significantly suppressed in the $\Delta recA$ strain compared to the wild
252 type strain after 4 hours of ampicillin exposure (Fig. 3D). More notably, the super-resolution
253 colocalization analysis revealed a significantly lower ratio of co-localization between the
254 chromosome and DNA Pol I in the $\Delta recA$ strain (Fig. 3E). Together, these findings
255 demonstrate that the RecA loss impairs DNA repair capacity beyond SOS regulon. This
256 repair deficiency contributes to genetic instability and is able to facilitate the rapid evolution
257 of antibiotic resistance through SOS-independent pathways.

258



259

260 **Figure 3. SOS-independent impairment of DNA repair in *ΔrecA* resistant isolates. (A)**
261 MICs of ampicillin were tested against the wild type strain, *ΔrecA* strain, and mutants lacking
262 specific genes from the SOS response after single exposures to ampicillin at 50 µg/mL for 8
263 hours. **(B)** Filament cell lengths in the wild type ($n=253$) and the *ΔrecA* strain ($n=216$) after
264 single treatments with ampicillin at 50 µg/mL. **(C)** Multinucleated filaments were observed in
265 the wild type (i) and the *ΔrecA* (ii) strain after single exposures to ampicillin at 50 µg/mL.
266 Purple: *E. coli* chromosome; green: DNA Pol I. **(D)** Relative fold changes of DNA Pol I in
267 the wild type and *ΔrecA* strain after single treatments with ampicillin at 50 µg/mL. **(E)** Co-
268 localization between the *E. coli* chromosome and DNA Pol I in the wild type and *ΔrecA*
269 strain after the single exposures to ampicillin at 50 µg/mL. Data is shown as mean \pm SEM.
270 Significant differences among different treatment groups are analyzed by independent t-test,
271 $*P < 0.05$, $**P < 0.01$, $***P < 0.001$, ns, no significance.
272

273 **Repression of antioxidative gene expression promotes the evolution of antibiotic
274 resistance in the *recA* mutant strain**

275 To further comprehend the fast evolution of β -lactam resistance observed in this study, we
276 investigated the gene expression changes induced by ampicillin using a comprehensive
277 transcriptome sequencing approach (total RNA-seq). Our analysis revealed significant
278 transcriptomic alterations in both the wild type and *ΔrecA* strain isolates following a single
279 treatment with ampicillin, compared to untreated controls (Fig. 4A). Specifically, we
280 identified changes in the expression of 161 and 248 coding sequences (with $\log_2\text{FC} > 2$ and P
281 value < 0.05) in the wild type and *ΔrecA* strains, respectively. Principal component analysis
282 (PCA) demonstrated a notable disparity in the effects of ampicillin on the *ΔrecA* strain
283 compared to the wild type strain (Fig. 4B). Additionally, Venn diagram analysis confirmed
284 that 138 and 225 genes were uniquely regulated by ampicillin exposure in the wild type and
285 *ΔrecA* strains, respectively (Fig. 4C).

286
287 To elucidate the differential expression of genes associated with specific biological functions,
288 we conducted Gene Ontology (GO) enrichment analyses (Figure 4-figure supplement 1A and
289 B) and Kyoto Encyclopedia of Genes and Genomes (KEGG) pathway analyses (Figure 4-
290 figure supplement 1C and D). Our findings indicate that ampicillin profoundly impacted
291 persistence pathways in the wild type strain, specifically affecting pathways related to
292 quorum sensing, flagellar assembly, biofilm formation, and bacterial chemotaxis (43,44).

293 Conversely, in the $\Delta recA$ strain, a distinct functional category associated with the oxidative
294 stress response exhibited significant and unique down-regulation. This category included
295 activities such as sulfate transporter activity, iron-sulfur cluster assembly, oxidoreductase
296 activity, and carboxylate reductase activity.

297

298 To identify specific genes showing significant fold changes ($\log_2 FC > 2$ and P value < 0.05),
299 we used volcano plots to visualize the comprehensive changes in gene expression across the
300 genome (Fig. 4D). We examined the transcription levels associated with the SOS response
301 system and found that the transcription of several proteins in the wild type strain can be
302 significantly induced by the single exposure to ampicillin, including *citB* and *dinB* (Fig. 4E).
303 However, in the *recA* mutant strain, antibiotic exposure does not affect the transcription
304 levels of any SOS system-related proteins, suggesting that antibiotic exposure induced the
305 SOS response in the wild type strain but not in the $\Delta recA$ strain. More importantly, we
306 discovered that the induction of the transcription level of the DNA Pol I was significantly
307 suppressed after the single treatment of ampicillin in the $\Delta recA$ strain compared with that in
308 the wild type strain (Fig. 4E). This is consistent with our imaging results and further supports
309 the notion that an SOS-independent evolutionary mechanism dominates the development of
310 antibiotic resistance in *recA* mutant *E. coli*.

311

312 Further, significant downregulation in the transcription of antioxidative-related genes in the
313 $\Delta recA$ strain was detected, including *cysJ*, *cysI*, *cysH*, *soda*, and *sufD* (Fig. 4F). This
314 downregulation suggested an excessive accumulation of reactive oxygen species (ROS) due
315 to compromised cell antioxidative defences. It has been previously reported that the induction
316 of mutagenesis can be stimulated by the overproduction of ROS during antibiotic
317 administration, leading to the evolution of antibiotic resistance both *in vivo* and *in vitro*
318 (22,23). Therefore, we hypothesized that elevated ROS levels facilitate the rapid evolution of
319 antibiotic resistance in the $\Delta recA$ strain by increasing genetic instability and enabling the
320 selection of resistant variants. To test it, we first examined the level of ROS generation in the
321 wild type and $\Delta recA$ strains treated with ampicillin for 8 hours by using the fluorescent probe
322 DCFDA/H2DCFDA. We found that ROS levels significantly increased in both the wild type
323 and $\Delta recA$ strain after 8 hours of ampicillin treatment. However, ROS levels in the $\Delta recA$
324 strain showed a significant further increase compared to the wild type strain (Fig. 4G).
325 Additionally, with the addition of 50 mM glutathione (GSH), a natural antioxidative
326 compound, no significant change in ROS levels was observed in either the wild type or $\Delta recA$

327 strain before and after ampicillin treatment (Fig. 4H). Further, we supplemented the wild type
328 and $\Delta recA$ strains with 50 mM GSH and treated them with ampicillin at a concentration of 50
329 μ g/ml for 8 hours. Remarkably, the addition of GSH prevented the development of resistance
330 to ampicillin in the $\Delta recA$ strain (Fig. 4I), without impairing the bactericidal effectiveness of
331 ampicillin (Fig. 4J).

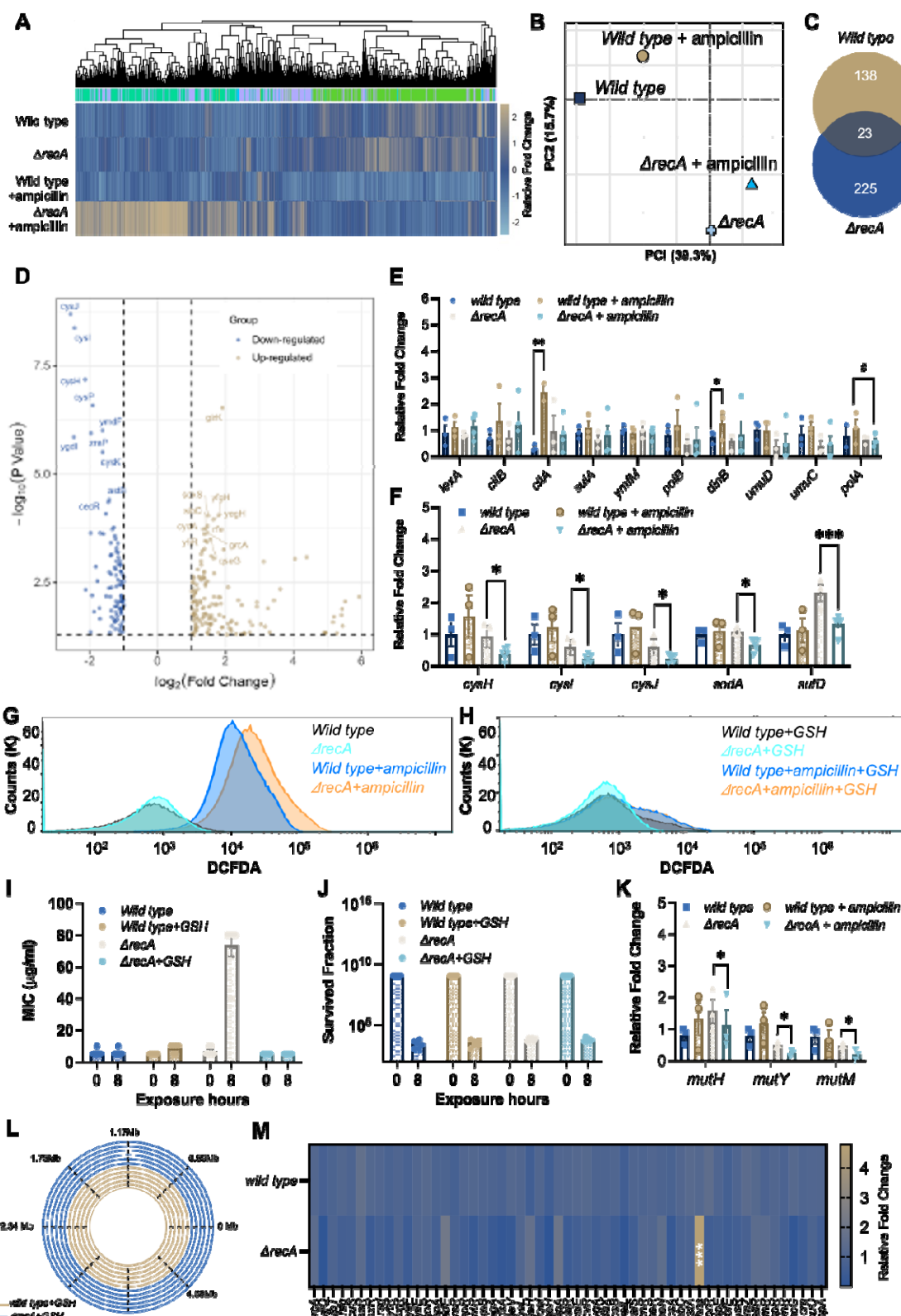
332

333 Apart from the SOS response, bacterial cells coordinate other DNA repair activities through a
334 network of regulatory pathways, including base excision repair (BER) (45-47). The excessive
335 generation of ROS results in elevated levels of deoxy-8-oxo-guanosine triphosphate (8-oxo-
336 dGTP), an oxidized form of dGTP that becomes both highly toxic and mutagenic upon
337 integration into DNA. The presence of 8-oxo-dG can induce SNP mutations, especially those
338 occurring in guanine, which can be actively rectified by the BER repair pathway (47).
339 Notably, BER glycosylases MutH and MutY can identify and repair these 8-oxo-dG-
340 dependent mutations; however, when MutY and MutH are inactivated, unrepaired 8-oxo-dG
341 can lead to the accumulation of SNP mutations within cells (47). As a result, we conducted a
342 further assessment of the transcription levels of the BER repair pathway in both the wild type
343 and $\Delta recA$ strain before and after a single exposure to ampicillin. We discovered that after an
344 8-hour treatment of ampicillin, three DNA repair-associated proteins, including MutH, MutY,
345 and MutM, were notably suppressed in the $\Delta recA$ strain (Fig. 4K).

346

347 Finally, we sequenced the surviving $\Delta recA$ isolates and found that the addition of GSH
348 inhibited drug resistance associated mutations in the $\Delta recA$ strain, which was detected in the
349 $\Delta recA$ resistant isolates including genes of the promoter of *ampC* and *acrB* (Fig. 4L). Given
350 the DNA repair impairment resulting in the generation of ROS, it would have been expected
351 for genes involved in the oxidative stress response to be induced in RecA-deficient cells.
352 However, the repression of antioxidative-related genes indicated the involvement of
353 transcriptional repressors that might be regulated by RecA. Consequently, we examined the
354 transcription levels of all transcriptional repressors in both the wild type and $\Delta recA$ strain.
355 Remarkably, we observed a significant upregulation of H-NS, a crucial transcriptional
356 repressor (Fig. 4M). This finding suggests that the upregulation of H-NS could potentially
357 contribute to the suppression of antioxidant gene expression in the $\Delta recA$ strain, thereby
358 promoting ROS accumulation and subsequent resistance evolution. Together, these findings
359 demonstrate that RecA deficiency not only impairs DNA repair but also suppresses the
360 oxidative stress response, leading to elevated ROS and increased mutational load. This

361 oxidative-genetic imbalance forms the basis for enhanced mutational supply in RecA-
362 deficient cells
363



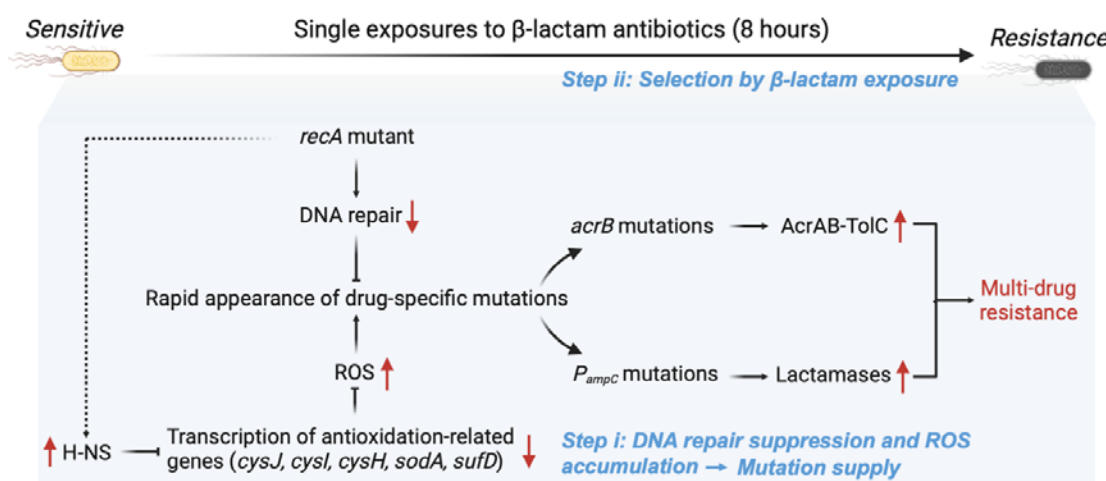
366 **Figure 4. Overaccumulation of ROS drives the fast evolution of multi-drug resistance in**
367 **the *ΔrecA* strain. (A)** Clustered heatmap of relative expression of coding sequences in the
368 wild type and *ΔrecA* strain with significant fold changes ($\log_2\text{FC} > 2$ and P value < 0.05). **(B)**
369 Principal-component analysis (PCA) of normalised read counts for all strains. **(C)** Venn
370 diagram of differentially expressed genes ($\log_2\text{FC} > 2$) after treatment with ampicillin at 50
371 $\mu\text{g}/\text{ml}$ for 8 hours in the wild type and *ΔrecA* strain. **(D)** The top 10 most differentially
372 expressed genes in the *ΔrecA* strain after the single treatment with ampicillin are labelled in
373 each plot. Blue dots indicate genes with a significant downregulation compared to the
374 untreated control ($\log_2\text{FC} > 2$ and P value < 0.05), and yellow dots indicate genes with a
375 significant upregulation compared to the untreated control ($\log_2\text{FC} > 2$ and P value < 0.05).
376 **(E)** Levels of transcription of SOS response system-associated genes and gene *polA* in the
377 wild type and *ΔrecA* strain after single exposures to ampicillin for 8 hours. **(F)** Levels of
378 transcription of different antioxidative associated genes in the wild type and *ΔrecA* strain
379 after single exposures to ampicillin for 8 hours. **(G)** ROS levels were measured by flow
380 cytometry before and after 8 hours of ampicillin treatment (50 $\mu\text{g}/\text{mL}$) in the wild type and
381 *ΔrecA* strains. **(H)** ROS levels were measured by flow cytometry in the wild type and *ΔrecA*
382 strains before and after 8 hours of ampicillin treatment at 50 $\mu\text{g}/\text{mL}$ with the addition of GSH
383 (50 mM). **(I)** The addition of 50 mM antioxidative compound GSH prevented the evolution
384 of antibiotic resistance to ampicillin in the *ΔrecA* strain treated with ampicillin at 50 $\mu\text{g}/\text{ml}$
385 for 8 hours. **(J)** Survival fraction after a single exposure to ampicillin at 50 $\mu\text{g}/\text{ml}$ for 8 hours
386 in the wild type and the *ΔrecA* strain with or without the addition of GSH at 50 mM. **(K)**
387 Levels of transcription of proteins involved in the BER DNA repair system in the wild type
388 and *ΔrecA* strain after single exposures to ampicillin for 8 hours. **(L)** Whole genome
389 sequencing confirms undetectable DNA mutations in the wild type and *ΔrecA* strain treated
390 with single exposures to ampicillin with the addition of GSH at 50 mM for 8 hours. **(M)**
391 Transcription levels of all transcriptional repressors in the wild type and *ΔrecA* strain after
392 single treatments with ampicillin for 8 hours. Total RNA-seq was performed with three
393 repeats in each group. Each experiment was independently repeated at least six times, and the
394 data are shown as mean \pm SEM. Significant differences among different treatment groups
395 are analyzed by independent t-test, $*P < 0.05$, $**P < 0.01$, $***P < 0.001$, $\#P < 0.05$.

396

397 **Discussion**

398 In this study, we challenge the prevailing view that disabling RecA and thereby inhibiting the
399 SOS response can prevent bacteria from developing antibiotic resistance (10). While the SOS
400 response and RecA have been extensively studied for their roles in antibiotic resistance
401 evolution (48), we observed a remarkably fast and stable evolution of multidrug resistance in
402 the *E. coli* Δ recA strains following a single exposure to β -lactam antibiotics. This
403 phenomenon cannot be explained by canonical SOS-driven mutagenesis (49), but instead
404 reflects the interplay of two distinct evolution forces: RecA loss increases mutational supply
405 through DNA repair suppression and ROS accumulation, while antibiotic-induced lethal
406 stress provides a selective environment that promotes the expansion of rare and resistance-
407 conferring variants (Fig. 5).

408



409

410 **Figure 5. Mechanism of rapid development of multidrug resistance in the *recA* mutant**
411 ***E. coli* strain.** Deletion of *recA* impairs DNA damage repair and upregulates the
412 transcription of the global repressor H-NS, though the mechanism of this regulation remains
413 unclear. Elevated H-NS levels repress the expression of multiple antioxidant-related genes
414 (*cysI*, *cysJ*, *cysH*, *sodA*, *sufD*), leading to excessive accumulation of ROS. The resulting
415 oxidative stress increases the overall mutational burden. Upon single exposure to β -lactam
416 antibiotics, drug-resistant subpopulations carrying specific mutations, such as in *acrB* or
417 *PampC*, are selectively enriched, ultimately driving the rapid emergence of multidrug
418 resistance. This process reflects a two-step mechanism involving enhanced mutational supply
419 and subsequent selection under antibiotic pressure.

420

421 To determine whether antibiotic exposure in Δ recA cells directly induces mutations or
422 selectively enriches resistant variants, we combined statistical modelling, fluctuation analysis,

423 and whole-genome sequencing. Although mutation rates estimated by maximum likelihood
424 were moderately elevated in $\Delta recA$ cells after ampicillin treatment, the mutation frequency
425 distributions were highly right-skewed and deviated from Poisson expectations, a hallmark of
426 clonal selection rather than uniform and population-wide mutagenesis. These findings align
427 with the classical Luria-Delbrück framework and indicate that resistance evolution in $\Delta recA$
428 is primarily driven by selection (29). However, our data also demonstrate that the mutational
429 supply is enhanced in this background due to antibiotic-induced oxidative stress and impaired
430 DNA repair, which together increase the likelihood that resistance-conferring mutations arise
431 and persist. Thus, this process reflects a selection-dominated evolutionary trajectory
432 facilitated by stress-enhanced mutagenesis, rather than classical induced mutation or selection
433 on pre-existing variants.

434

435 Mechanistically, our data reveal that RecA plays broader roles in genome stability beyond its
436 function in SOS activation. Disruption of individual SOS components, including *lexA*, *citA/B*,
437 or translesion polymerases, did not recapitulate the $\Delta recA$ -specific resistance phenotype.
438 Instead, $\Delta recA$ strains exhibited suppression of DNA Pol I. and key BER genes, such as *mutH*,
439 *mutY*, and *mutM*, confirming that RecA is essential for the maintenance of repair fidelity
440 under stress conditions. This defect likely enables ROS-induced DNA lesions to persist and
441 become fixed as mutations.

442

443 In parallel, we identified a striking repression of antioxidative stress response genes in $\Delta recA$
444 strains exposed to ampicillin, including *cysJIH*, *sodA*, and *sufD*. This transcriptional
445 suppression was associated with markedly elevated ROS levels. Crucially, supplementation
446 with the antioxidant GSH reversed both ROS accumulation and the emergence of resistance,
447 without impairing the bactericidal activity of ampicillin. This decouples the mutagenic and
448 lethal effects of ROS, and highlights ROS as a driver of mutational supply rather than
449 survival.

450

451 To explore the transcriptional basis for oxidative dysregulation, we examined global
452 repressors and discovered that *hns* was significantly upregulated in $\Delta recA$ strains after
453 ampicillin exposure. H-NS is a known transcriptional silencer of stress response genes,
454 including those involved in redox regulation (50,51). We propose that RecA deficiency may
455 lead to H-NS derepression, thereby silencing antioxidant defences, exacerbating ROS
456 accumulation, and enabling mutation accumulation under stress. Although previous findings

457 report that H-NS can down-regulate the transcriptional expression of *cysIJH* through the
458 mediation of *cysB* (52,53), the mechanistic relationship between RecA and H-NS regulation
459 remains to be experimentally validated.

460

461 More broadly, our findings highlight the repair-redox axis as a central regulator of bacterial
462 evolvability. Rather than solely targeting bacterial growth or survival, future antimicrobial
463 strategies might focus on constraining mutational potential. For example, co-administration
464 of antioxidants or repair stabilizers could buffer stress-induced mutagenesis without
465 compromising antibiotic efficacy, which has been a concept already under exploration in
466 cancer therapeutics (54,55).

467

468 Clinically, the emergence of *acrB* mutations and enhanced activity of the AcrAB-TolC efflux
469 pump in Δ *recA* strains recapitulates known multidrug resistance pathways. These
470 observations raise concerns for therapies combining DNA repair inhibitors with ROS-
471 inducing antibiotics or anticancer drugs (56). Our data suggest that such combinations may
472 inadvertently promote resistance evolution, particularly in immunocompromised patients or
473 during chemotherapy.

474

475 Finally, ROS-driven mutagenesis and repair suppression are not unique to β -lactams.
476 Antimicrobial technologies such as antimicrobial photodynamic therapy (aPDT) and cold
477 atmospheric plasma (CAP) (57,58) also rely on oxidative stress. In RecA-deficient or stress-
478 sensitized bacteria, these approaches may risk accelerating resistance evolution unless
479 accompanied by safeguards that preserve genomic integrity. Thus, maintaining the
480 transcription of genes involved in the oxidative stress defence or combining antibiotics
481 represents a promising strategy to prevent ROS-driven mutagenesis and thereby limit the
482 evolutionary emergence of resistance during antimicrobial therapy.

483

484 **Acknowledgements**

485 This work was supported by the Australian Research Council (ARC grant no: APP1165135),
486 Science and Technology Innovation Commission of Shenzhen (KQTD20170810110913065),
487 Australia China Science and Research Fund Joint Research Centre for Point-of-Care Testing
488 (ACSRF658277, SQ2017YFGH001190).

489

490 **Competing interests**

491 The authors declare that they have no competing interests.

492

493 **Data and materials availability**

494 All data are available in the main text or the supplementary materials.

495

496 **Reference**

- 497 1. Rebecca S. Antimicrobial-Induced DNA Damage and Genomic Instability in Microbial
498 Pathogens. *PLOS Pathogens*. **11**, e1004678 (2015).
- 499 2. Kohanski MA, Dwyer DJ, Hayete B, Lawrence CA, Collins JJ. A common mechanism of
500 cellular death induced by bactericidal antibiotics. *Cell*. **7**, 130 (5): 797-810 (2007).
- 501 3. Baquero F, Levin BR. Proximate and ultimate causes of the bactericidal action of
502 antibiotics. *Nat Rev Microbiol*. **19** (2): 123-132 (2021).
- 503 4. Žgur-Bertok D. DNA Damage Repair and Bacterial Pathogens. *PLOS Pathogens*. **9** *PLOS*
504 *Pathogens*, e1003711 (2013).
- 505 5. Dale B. Wigley. Bacterial DNA Repair: Recent Insights into The Mechanism of RecBCD,
506 AddAB and AdnAB. *Nature Reviews Microbiology*. **11**, 9-13 (2013).
- 507 6. Harms A, Maisonneuve E, Gerdes K. Mechanisms of Bacterial Persistence during Stress
508 and Antibiotic Exposure. *Science*. **354**, aaf4268 (2016).
- 509 7. Katarzyna H. Maslowska, Karolina Makiela-Dzbenska, Iwona J. Fijalkowska. The SOS
510 System: A Complex and Tightly Regulated Response to DNA Damage. *Environ Mol*
511 *Mutagen*. **60**, 368-384 (2019).
- 512 8. Michael M. Cox. Motoring Along with the Bacterial RecA Protein. *Nature Reviews*
513 *Molecular Cell Biology*. **8**, 127-138 (2007).
- 514 9. Barrett, T.C., Mok, W.W.K., Murawski, A.M. et al. Enhanced antibiotic resistance
515 development from fluoroquinolone persisters after a single exposure to antibiotic. *Nat*
516 *Commun*. **10**, 1177 (2019).
- 517 10. Athanasia Pavlopoulou. RecA: A Universal Drug Target in Pathogenic Bacteria.
518 *Frontiers in Bioscience*. **23**, 36-42 (2018).
- 519 11. Mercolino J, Lo Sciuto A, Spinnato MC, Rampioni G, Imperi F. RecA and Specialized
520 Error-Prone DNA Polymerases Are Not Required for Mutagenesis and Antibiotic
521 Resistance Induced by Fluoroquinolones in *Pseudomonas aeruginosa*. *Antibiotics (Basel)*.
522 **11**, 3, 325 (2022).

523 12. Miller C, Thomsen LE, Gaggero C, Mosseri R, Ingmer H, Cohen SN. SOS response
524 induction by beta-lactams and bacterial defense against antibiotic lethality. *Science*. **305**
525 (5690), 1629-31 (2004).

526 13. Jahn LJ, Munck C, Ellabaan MMH, Sommer MOA. Adaptive Laboratory Evolution of
527 Antibiotic Resistance Using Different Selection Regimes Lead to Similar Phenotypes and
528 Genotypes. *Front Microbiol*. **8**:816 (2017).

529 14. Levin-Reisman I, Ronin I, Gefen O, Braniss I, Shores N, Balaban NQ. Antibiotic
530 Tolerance Facilitates the Evolution of Resistance. *Science*. **355**, 826-830 (2017).

531 15. Dwyer DJ, Kohanski MA, Hayete B, Collins JJ. Gyrase inhibitors induce an oxidative
532 damage cellular death pathway in *Escherichia coli*. *Mol Syst Biol*. **3**: 91 (2007).

533 16. Kohanski MA, Dwyer DJ, Hayete B, Lawrence CA, Collins JJ. A common mechanism of
534 cellular death induced by bactericidal antibiotics. *Cell*. **7**, 130(5): 797-810 (2007).

535 17. Luan, G, Hong, Y, Drlica, K, and Zhao, X. Suppression of reactive oxygen species
536 accumulation accounts for paradoxical bacterial survival at high quinolone concentration.
537 *Antimicrob. Agents Chemother*. **62**: e01617-e01622 (2018).

538 18. Zhao X, Drlica K. Reactive oxygen species and the bacterial response to lethal stress.
539 *Curr Opin Microbiol*. **21**, 1-6 (2014).

540 19. Zhao X, Hong Y, Drlica K. Moving forward with reactive oxygen species involvement in
541 antimicrobial lethality. *J Antimicrob Chemother*. **70** (3): 639-642 (2015).

542 20. Keren I, Wu Y, Inocencio J, Mulcahy LR, Lewis K. Killing by bactericidal antibiotics
543 does not depend on reactive oxygen species. *Science*. **339** (6124):1213-1216 (2013).

544 21. Imlay JA. Diagnosing oxidative stress in bacteria: not as easy as you might think. *Curr*
545 *Opin Microbiol*. **24**, 124-131 (2015).

546 22. Kohanski MA, DePristo MA, Collins JJ. Sublethal antibiotic treatment leads to multidrug
547 resistance via radical-induced mutagenesis. *Mol Cell*. **37**(3): 311-320 (2010).

548 23. Takahashi N, Gruber CC, Yang JH, Liu X, Braff D, Yashaswini CN, Bhubhanil S, Furuta
549 Y, Andreeescu S, Collins JJ, Walker GC. Lethality of MalE-LacZ hybrid protein shares
550 mechanistic attributes with oxidative component of antibiotic lethality. *Proc Natl Acad Sci*
551 *USA*. **114** (34): 9164-9169 (2017).

552 24. Andersson DI, Hughes D. Microbiological effects of sublethal levels of antibiotics. *Nat.*
553 *Rev. Microbiol*. **12**, 465-478 (2014).

554 25. Fridman, O., Goldberg, A., Ronin, I. et al. Optimization of lag time underlies antibiotic
555 tolerance in evolved bacterial populations. *Nature*, **513**, 418-421 (2014).

556 26. Reimer LG, Stratton CW, Reller LB. Minimum inhibitory and bactericidal concentrations
557 of 44 antimicrobial agents against three standard control strains in broth with and without
558 human serum. *Antimicrob Agents Chemother.*, **19**, 1050-1055 (1981).

559 27. Jones RN, Fuchs PC, Gerlach EH, Gavan TL. Piperacillin and carbenicillin; a
560 collaborative in vitro comparison against 10,838 clinical bacterial isolates. *Cleveland*
561 *Clinic Journal of Medicine*, **46**, 49-55 (1979).

562 28. Baquero F, Coque TM, Galán JC, Martínez JL, Cantón R. Evolutionary pathways and
563 trajectories in antibiotic resistance. *Clinical Microbiology Reviews*, **34**, e00050-19 (2021).

564 29. Luria SE, Delbrück M. Mutations of bacteria from virus sensitivity to virus resistance.
565 *Genetics*, **28**, 491-511 (1943).

566 30. Zheng Q. Progress of a half century in the study of the Luria–Delbrück distribution.
567 *Mathematical Biosciences*, **162**, 1-32 (1999).

568 31. Sarkar S, Ma WT, Sandri GVH. On fluctuation analysis: a new, simple and efficient
569 method for computing the expected number of mutants. *Genetica*, **85**, 173-179 (1992).

570 32. Foster PL. Stress-induced mutagenesis in bacteria. *Critical Reviews in Biochemistry and*
571 *Molecular Biology*, **42**, 373–397 (2007).

572 33. Toprak E, Veres A, Michel JB, Chait R, Hartl DL, Kishony R. Evolutionary paths to
573 antibiotic resistance under dynamically sustained drug selection. *Nat Genet.* **44** (1), 101-
574 105 (2011).

575 34. Kamiya H, Murata-Kamiya N, Iida E, Harashima H. Hydrolysis of oxidized nucleotides
576 by the *Escherichia coli* Orf135 protein. *Biochem Biophys Res Commun.* **288** (3): 499-502
577 (2001).

578 35. El Meouche I, Dunlop MJ.. Heterogeneity in Efflux Pump Expression Predisposes
579 Antibiotic-Resistant Cells to Mutation. *Science*. **362**, 686-690 (2018).

580 36. Jessica M. A. Blair et al. Molecular Mechanisms of Antibiotic Resistance. *Nature*
581 *Reviews Microbiology*. **13**, 42-51 (2015).

582 37. Simmons LA, Foti JJ, Cohen SE, Walker GC. The SOS regulatory network. *EcoSal Plus*.
583 5.4.3 (2008).

584 38. Ansari S, Walsh JC, Bottomley AL, Duggin IG, Burke C, Harry EJ. A newly identified
585 prophage-encoded gene, *ymfM*, causes SOS-inducible filamentation in *Escherichia coli*. *J*
586 *Bacteriol.* **15**, 203(11): e00646-20 (2015).

587 39. Monk M, Peacey M, Gross JD. Gross. Repair of Damage Induced By Ultraviolet Light in
588 DNA Polymerase-Defective *Escherichia Coli* Cells. *Journal of Molecular Biology*. **58**,
589 623-624 (1971).

590 40. Joyce CM, Grindley ND. Method for determining whether a gene of *Escherichia coli* is
591 essential: application to the *polA* gene. *J Bacteriol.* 158(2): 636-643 (1984).

592 41. Konrad EB, Lehman IR. A conditional lethal mutant of *Escherichia coli* K12 defective in
593 the 5' leads to 3' exonuclease associated with DNA polymerase I. *Proc Natl Acad Sci.*
594 71(5): 2048-2051 (1974).

595 42. Justice SS, Hunstad DA, Cegelski L, Hultgren SJ. Morphological Plasticity as a Bacterial
596 Survival Strategy. *Nature Review Microbiology.* 6, 162-168 (2008).

597 43. Helaine S, Kugelberg E. Bacterial Persisters: Formation, Eradication, and Experimental
598 Systems. *Trends in Microbiology.* 22, 417-424 (2014).

599 44. Amy L. Spoering, Kim Lewis. Biofilms and Planktonic Cells of *Pseudomonas*
600 *Aeruginosa* Have Similar Resistance to Killing by Antimicrobials. *J. Bacteriol.* 183, 6746-
601 6751 (2001).

602 45. Foti JJ, Devadoss B, Winkler JA, Collins JJ, Walker GC. Oxidation of the guanine
603 nucleotide pool underlies cell death by bactericidal antibiotics. *Science.* 336(6079): 315-
604 319 (2012).

605 46. DNA repair and mutagenesis (2nd ed.). *ASM Press* (2005).

606 47. Hahm JY, Park J, Jang ES, Chi SW. 8-Oxoguanine: from oxidative damage to epigenetic
607 and epitranscriptional modification. *Exp Mol Med.* 54(10): 1626-1642 (2022).

608 48. Pavlopoulou A. RecA: A Universal Drug Target in Pathogenic Bacteria. *Frontiers in*
609 *Bioscience.* 23, 36-42 (2018).

610 49. Janion C. Inducible SOS response system of DNA repair and mutagenesis in *Escherichia*
611 *coli*. *International Journal of Biological Sciences*, 4, 338-344 (2008).

612 50. Dorman CJ. H-NS: a universal regulator for a dynamic genome. *Nat Rev Microbiol.* 2
613 (5):391-400 (2004).

614 51. Bracco L, Kotlarz D, Kolb A, Diekmann S, Buc H. Synthetic curved DNA sequences can
615 act as transcriptional activators in *Escherichia coli*. *EMBO J.* 8 (13):4289-96 (1989).

616 52. Álvarez R, Neumann G, Frávega J, Díaz F, Tejías C, Collao B, Fuentes JA, Paredes-Sabja
617 D, Calderón IL, Gil F. CysB-dependent upregulation of the *Salmonella* Typhimurium
618 cysJIH operon in response to antimicrobial compounds that induce oxidative stress.
619 *Biochem Biophys Res Commun.* 458 (1):46-51 (2015).

620 53. Ishihama A, Shimada T. Hierarchy of transcription factor network in *Escherichia coli* K-
621 12: H-NS-mediated silencing and Anti-silencing by global regulators. *FEMS Microbiol*
622 *Rev.* 45 (6):fuab032 (2021).

623 54. Aguilera A, Gómez-González B. Genome instability: a mechanistic view of its causes and
624 consequences. *Nature Reviews Genetics*, **9**, 204-217 (2008).

625 55. Klinakis A, Karagiannis D, Rampias T. Targeting DNA repair in cancer: current state and
626 novel approaches. *Cellular and Molecular Life Sciences*, **77**, 677-703 (2020).

627 56. Wang M, Chen S, Ao D. Targeting DNA repair pathway in cancer: mechanisms and
628 clinical application. *MedComm*, **2**, 654-691 (2021).

629 57. Wilson, BC, and Patterson, MS. The physics, biophysics and technology of photodynamic
630 therapy. *Phys. Med. Biol.* **53**, R61-R109 (2008).

631 58. Vatansever F, de Melo WC, Avci P, Vecchio D, Sadasivam M, Gupta A, Chandran R,
632 Karimi M, Parizotto NA, Yin R, Tegos GP, Hamblin MR. Antimicrobial strategies
633 centered around reactive oxygen species-bactericidal antibiotics, photodynamic therapy,
634 and beyond. *FEMS Microbiol Rev.* **37**(6): 955-989 (2013).

635 59. Ghodke H, Paudel BP, Lewis JS, Jergic S, Gopal K, Romero ZJ, Wood EA, Woodgate R,
636 Cox MM, van Oijen AM. Spatial and temporal organization of RecA in the *Escherichia*
637 *coli* DNA-damage response. *Elife*, **8**: e42761 (2019).

638 60. Eric M. Scholar, William B. Pratt. *The Antimicrobial Drugs*. Oxford University Press.

639 61. A. Gutierrez, L. Laureti, S. Crussard, H. Abida, A. Rodríguez-Rojas, J. Blázquez, Z.
640 Baharoglu, D. Mazel, F. Darfeuille, J. Vogel, I. Matic, β -Lactam antibiotics promote
641 bacterial mutagenesis via a RpoS-mediated reduction in replication fidelity. *Nat. Commun.*
642 **4**, 1610 (2013).

643 62. Kirill A. Datsenko, Barry L. Wanner. One-Step Inactivation of Chromosomal Genes in
644 *Escherichia Coli* K-12 Using PCR Products. *Proc Natl Acad Sci.* **97**, 6640-6645 (2000).

645 63. Baba T, Ara T, Hasegawa M, Takai Y, Okumura Y, Baba M, Datsenko KA, Tomita M,
646 Wanner BL, Mori H. Construction of *Escherichia Coli* K-12 In-Frame, Single-Gene
647 Knockout Mutants: The Keio Collection. *Mol Syst Biol*, **2**, 2006.0008 (2006).

648 64. Van der Auwera GA & O'Connor BD. Genomics in the Cloud: Using Docker, GATK,
649 and WDL in Terra (1st Edition). *O'Reilly Media*. (2020).

650 65. Cingolani P, Platts A, Wang le L, Coon M, Nguyen T, Wang L, Land SJ, Lu X, Ruden
651 DM. A program for annotating and predicting the effects of single nucleotide
652 polymorphisms, SnpEff: SNPs in the genome of *Drosophila melanogaster* strain w1118;
653 iso-2; iso-3. *Fly (Austin)*. **6**, 2, 80-92 (2012)

654 66. Liao Y, Smyth GK, Shi W. The R package Rsubread is easier, faster, cheaper and better
655 for alignment and quantification of RNA sequencing reads. *Nucleic Acids Res.* **30**, 923
656 (2019).

657 67. Love MI, Huber W, Anders S. Moderated estimation of fold change and dispersion for
658 RNA-seq data with DESeq2. *Genome Biol.* **15**, 550 (2014).

659 68. Risso D, Ngai J, Speed TP, Dudoit S. Normalization of RNA-seq data using factor
660 analysis of control genes or samples. *Nat Biotechnol* **32**, 896-902 (2014).

661 69. Su QP, Zhao ZW, Meng L, Ding M, Zhang W, Li Y, Liu M, Li R, Gao YQ, Xie XS, Sun
662 Y. Superresolution Imaging Reveals Spatiotemporal Propagation of Human Replication
663 Foci Mediated By CTCF-Organized Chromatin Structures. *Proceedings of the National
664 Academy of Sciences.* **117**, 15036-15046 (2020).

665 70. Wang G, Li Y, Wang P, Liang H, Cui M, Zhu M, Guo L, Su Q, Sun Y, McNutt MA, Yin
666 Y. PTEN Regulates RPA1 and Protects DNA Replication Forks. *Cell Res.* **25**, 1189-1204
667 (2015).

668 71. Huang B, Wang W, Bates M, Zhuang X. Three-Dimensional Super-Resolution Imaging
669 by Stochastic Optical Reconstruction Microscopy. *Science.* **319**, 810-813 (2008).

670 72. Levet F, Hosy E, Kechkar A, Butler C, Beghin A, Choquet D, Sibarita JB. SR-tesseler: A
671 Method to Segment and Quantify Localization-Based Super-Resolution Microscopy Data.
672 *Nat. Methods.* **12**, 1065–1071 (2015).

673

674 **Materials and Methods**

675 **Bacterial strains, medium and antibiotics**

676 Bacterial strains and plasmids used in this work are described in Table S2 and Table S3.
677 Luria-Bertani (LB) was used as broth or in agar plates. *E. coli* cells were grown in LB liquid
678 medium or on LB agar (1.5% w/v) plates at 37°C, unless stated otherwise, antibiotics were
679 supplemented, where appropriate. Antibiotic stock solutions were prepared by dissolving
680 antibiotics in MilliQ filter sterilising, including ampicillin (50 mg/mL), penicillin G (100
681 mg/mL), carbenicillin (20 mg/mL), kanamycin (50 mg/mL) and tetracycline (10 mg/mL).
682 Chloramphenicol stock solution was prepared in 95% EtOH (25 mg/mL). Antibiotic solutions
683 were stored at -20°C (long-term) or 4°C (short-term).

684

685 **Treatment with antibiotics to induce evolutionary resistance**

686 For the single exposure to antibiotic experiment, an overnight culture (0.6 mL; 1 x 10⁹
687 CFU/mL cells) was diluted 1:50 into 30 mL LB medium supplemented with antibiotics (50
688 µg/mL ampicillin, 1 mg/mL penicillin G, or 200 µg/mL carbenicillin) and incubated at 37°C
689 with shaking at 250 rpm for 0, 2, 4, 6 and 8 hours, respectively. After each treatment, the

690 antibiotic-containing medium was removed by washing twice (20 min centrifugation at 1500
691 g) in fresh LB medium (See Fig. 1A for method overview).

692

693 To test resistance, the surviving isolates were first resuspended in 30 mL LB medium and
694 grown overnight at 37°C with shaking at 250 rpm. The regrown culture was then plated onto
695 LB agar and incubated overnight at 37°C. Single colonies were isolated and grown in LB
696 medium for 4-6 hours at 37°C with shaking at 250 rpm, which were then used to test the
697 resistance or stored at -80°C for future use.

698

699 For the ALE antibiotic treatment experiments, an overnight culture (0.6 mL; 1×10^9 CFU/mL
700 cells) was diluted 1:50 into 30 mL LB medium supplemented with 50 µg/mL ampicillin and
701 incubated at 37°C with shaking at 250 rpm for 4.5 hours. After treatment, the antibiotic-
702 containing medium was removed by washing twice (20 min centrifugation at 1500 g) in a
703 fresh LB medium. The remaining pellet was resuspended in 30 mL LB medium and grown
704 overnight at 37°C with shaking at 250 rpm. Ampicillin treatment was applied to the regrown
705 culture and repeated until resistance was established, as confirmed by MIC measurement.

706

707 **Antibiotic susceptibility testing**

708 The susceptibility of *E. coli* cells to antibiotics was measured using minimum inhibitory
709 concentration (MIC) testing (60). In brief, overnight cultures were diluted and incubated at
710 37°C for 4-6 hours with shaking at 250 rpm. Cells were then diluted 1:100 and incubated
711 with increasing concentrations of antibiotics in the Synergy HT BioTek plate reader (BioTek
712 Instruments Inc., USA) at 37°C for 16 hours. It was programmed to measure the OD hourly at
713 595 nm (Gen5 software, BioTek Instruments Inc., USA). The minimum inhibitory
714 concentration was determined as the concentration of antibiotic where no visible growth was
715 observed.

716

717 **Survival assays**

718 Overnight cultures of *E. coli* were prepared from single colonies in LB medium and
719 incubated at 37°C with shaking (250 rpm). The overnight cultures were diluted 1:50 in fresh
720 LB medium containing 50 µg/mL ampicillin to initiate antibiotic treatment. Cultures were
721 incubated at 37°C for the indicated times under shaking conditions. Following treatment,
722 cells were collected by centrifugation (1500 g, 20 minutes), and the antibiotic-containing
723 medium was removed by washing twice with fresh LB medium. Serial dilutions of the

724 washed cultures were prepared, and 25 μ L of each dilution was plated onto LB agar plates.
725 Plates were incubated overnight at 37°C, and CFUs were counted the following day to
726 evaluate bacterial survival rates.

727

728 **Mutation frequency and fluctuation analysis**

729 Overnight cultures inoculated from single colonies in LB medium were diluted 1:1,000,000
730 and incubated at 37°C with shaking until the OD₆₀₀ reached to 1~1.3. This extreme dilution
731 minimizes the presence of pre-existing stationary phase mutants and allows *de novo* mutation
732 events to occur during exponential growth. For each biological condition, 96 independent
733 parallel cultures were prepared to perform a fluctuation analysis. The total number of colony-
734 forming units per ml (CFU/ml) was determined by plating on LB agar. To identify
735 rifampicin-resistant mutants, the remaining culture volume was centrifuged and plated on LB
736 agar containing rifampicin (100 μ g/mL). LB plates were incubated for 24 hours at 37°C and
737 selective plates were incubated for 48-72 hours at 37°C (61).

738

739 The mutation frequency was calculated as the ratio of CFU/ml on rifampicin-containing
740 plates to CFU/ml on non-selective LB plates for each culture. Distributions of mutation
741 frequencies across replicate cultures were plotted, and deviations from Poisson expectations
742 were assessed by model fitting.

743

744 To estimate the mutation rate (mutations per culture), maximum likelihood estimation (MLE)
745 was applied using the Ma-Sandri-Sarkar algorithm implemented in the FALCOR toolset
746 (<https://www.keshavsingh.org/protocols/FALCOR.html>). The inferred mutation rate
747 distributions were compared across treatment conditions, and non-Poisson distributions
748 indicative of jackpot cultures were further analysed using fluctuation test-based inference
749 following the Luria–Delbrück framework (29).

750

751 **Construction of *recA* deletion mutant**

752 Lambda Red recombination was used to generate the gene *recA* deletion in the *E. coli* K-12
753 strain, followed by previously reported methods with modifications (62,63). Primers (*recA-*
754 *FWD* and *recA-REV*, Table S4) were designed approximately 50 bp upstream and
755 downstream to the gene *recA* on the chromosome to amplify the tetracycline cassette as well
756 as the flanking DNA sequence needed for homologous recombination. Phusion polymerase
757 (NEB) was used to amplify the DNA sequence (Table S4), and the reaction was cleaned up

758 using a PureLink™ PCR purification kit (ThermoFisher Scientific) as per the manufacturer's
759 instructions. Electro-competent *E. coli* MG1655 containing the recombinase plasmid pKD46
760 was transformed with 50 ng of amplified DNA a 30°C. The transformation was plated onto
761 LB agar plates containing 10 µg/mL tetracycline and incubated overnight at 37°C. PCR was
762 used to confirm the insertion of the tetracycline resistance cassette at the correct site on the
763 chromosome using primers upstream and downstream to the gene *recA*. The newly
764 constructed mutant strains were cured of plasmid pKD46 by incubating LB streak plates at
765 42°C overnight. Loss of the plasmid was confirmed by lack of ampicillin sensitivity on LB
766 agar plates. Mutant strains were made electro-competent, and 50 µL of cells were
767 transformed with plasmid pCP20 and incubated on 100 µg/mL ampicillin plates at 30°C
768 overnight. A few colonies were then restreaked onto LB plates and incubated overnight at
769 42°C. PCR products confirmed the loss of cassette and plasmid.

770

771 **β-lactamase assay**

772 The amount of β-lactamase was measured using a β-lactamase Activity Assay Kit (Sigma-
773 Aldrich, US). Briefly, cells were collected by centrifugation at 10,000 g for 10 min, and the
774 pellet was resuspended with 5 µL of assay buffer per mg of sample. Then, 48 µL of the
775 sample was mixed with 2 µL of nitrocefin. The β-Lactamase activity was monitored by
776 measuring the absorbance at 490 nm for 30 min at 28°C. The level of β-lactamase was
777 determined by the absorbance at OD₃₉₀.

778

779 **Whole genome sequencing**

780 Resistant clones were isolated by selection using LB agar plates with the supplementation of
781 ampicillin at 50 µg/mL, and non-resistant clones were isolated from the LB agar plates
782 without the supplementation of antibiotics. Chromosomal DNA was extracted and purified
783 using the PureLink™ Genomic DNA mini kit following the manufacturer's instructions
784 (ThermoFisher Scientific). Whole genome sequencing (WGS) was conducted following the
785 Nextera Flex library preparation kit process (Illumina). Briefly, genomic DNA was
786 quantitatively assessed using Quant-iT picogreen dsDNA assay kit (Invitrogen, USA). The
787 sample was normalised to the concentration of 1 ng/µL. 10 ng of DNA was used for library
788 preparation. After tagmentation, the tagmented DNA was amplified using the facility's
789 custom-designed i7 or i5 barcodes, with 12 cycles of PCR. The quality control for the
790 samples was done by sequencing a pool of samples using MiSeq V2 nano kit - 300 cycles.
791 After library amplification, 3 µL of each library was pooled into a library pool. The pool was

792 then cleaned up using SPRI beads following the Nextera Flex clean-up and size selection
793 protocol. The pool was then sequenced using a MiSeq V2 nano kit (Illumina, USA). Based on
794 the sequencing data generated, the read count for each sample was used to identify the failed
795 libraries (i.e., libraries with less than 100 reads).

796

797 Moreover, libraries were pooled at different amounts based on the read count to ensure equal
798 representation in the final pool. The final pool was sequenced on Illumina NovaSeq 6000 Xp
799 S4 lane, 2 × 150 bp. WGS read quality was assessed using FASTQC (version 0.11.5) and
800 trimmed using Trimmomatic (version 0.36) with default parameters and trimmed of adaptor
801 sequences (TruSeq3 paired-ended). Reads were aligned to the *E. coli* MG1655 genome
802 (http://bacteria.ensembl.org/Escherichia_coli_str_k_12_substr_mg1655_gca_000005845/Info_Index/, assembly ASM584v2) and then analysed variants following GATK Best Practices for
803 Variant Discovery (HaplotypeCaller) (64). Further genome variant annotation was conducted
804 using the software SnpEff (65).

805

806

807 **Global transcriptome sequencing**

808 After ampicillin treatment for 0 and 8, surviving isolates were immediately washed and
809 harvested for global transcriptome sequencing. Total RNA was extracted from the cell pellets
810 using a PureLink RNA mini kit (Invitrogen) as per the manufacturer's instructions. The
811 global transcriptome sequencing was processed and analysed by Genewiz, Jiangsu, China.
812 Primers used in this work are listed in Table S4. RNA-Seq read quality was assessed using
813 FASTQC and trimmed using Trimmomatic with default parameters. Reads were aligned to
814 the *E. coli* MG1655 genome

815 (http://bacteria.ensembl.org/Escherichia_coli_str_k_12_substr_mg1655_gca_000005845/Info_Index/, assembly ASM584v2) and then counted using the RSubread aligner with default
816 parameters (66). After mapping, differential expression analysis was carried out using strand-
817 specific gene-wise quantification using the DESeq2 package (67). Further normalisation was
818 conducted using RUVSeq and the RUV correction method, with $k = 1$ to correct for batch
819 effects, using replicate samples to estimate the factors of unwanted variation (68). Absolute
820 counts were transformed into standard z-scores for each gene over all treatments, that is,
821 absolute read for a gene minus mean read count for that gene over all samples and then
822 divided by the standard deviation for all counts over all samples. Genes with an adjusted *P*
823 value (P_{adj}) of ≤ 0.05 were considered differentially expressed. PseudoCAP analysis was

825 conducted by calculating the percentage of genes in each classification that were
826 differentially expressed ($\log_2\text{FC} \geq \pm 2$, $P_{\text{adj}} \leq 0.05$).

827

828 **ROS measurement**

829 Intracellular ROS accumulation was measured using the Cellular ROS Assay Kit (Abcam,
830 ab113851) according to the manufacturer's protocol. Overnight cultures of both wild type and
831 $\Delta recA$ strains were grown in LB medium. Cells were treated with 50 $\mu\text{g/mL}$ ampicillin for 8
832 hours at 37°C with shaking (250 rpm). After the treatment, cells were washed twice with 1x
833 buffer to remove residual antibiotics and debris. The collected cells were resuspended in 1x
834 buffer and incubated with the fluorescent ROS probe DCFDA (2',7'-dichlorofluorescin
835 diacetate)/H2DCFDA at a final concentration of 10 μM for 30 minutes at 37°C in the dark to
836 prevent probe degradation.

837

838 After incubation, 500 μL of the stained cells were immediately analysed using a CytoFLEX
839 LX flow cytometer (Beckman Coulter). Fluorescence was detected in the FITC channel
840 (excitation at 488 nm, emission at 525 nm). Data were analysed using FlowJo software
841 (Version X, Tree Star Inc.), with fluorescence intensity serving as an indicator of intracellular
842 ROS levels. Appropriate controls, including unstained cells and cells without ampicillin
843 treatment, were included to ensure accurate ROS measurement.

844

845 **Single-molecule localisation imaging and data analysis**

846 Single-molecule localisation imaging was performed on a custom-built Stochastic Optical
847 Reconstruction Microscope (STORM) with an Olympus IX81 microscope frame, a 100x
848 magnification NA 1.45 objective (Olympus) and an EMCCD camera (DU-897, Andor) as
849 described previously (69-71). In summary, 35 mm cell culture dishes (0.17 mm No.1
850 coverglass) were cleaned with 1 M KOH for 30 minutes in an ultrasonic cleaning machine,
851 followed by three washes with MilliQ water. The dishes were air-dried with high-purity
852 nitrogen blowing and sterilised by UV exposure for 30 minutes. *E. coli* cells were fixed with
853 NaPO4 (30 nM), formaldehyde (2.4%), and glutaraldehyde (0.04%) at room temperature for
854 15 minutes, followed by 45 minutes on ice. Samples were then centrifuged to collect the
855 pellet cells, and the supernatant was discarded. Cell pellets were washed twice with
856 phosphate-buffered saline (PBS), pH 7.4. Cells were resuspended in 200 μL of GTE buffer
857 and kept on ice until 200 μL was placed onto the coverslip bottom of the cleaned 35 mm

858 culture dish. To label the bacterial chromosome, a Click-iT EdU kit was used prior to
859 fixation following the manufacturer's instruction (ThermoFisher) and as described before. To
860 label DNA polymerase I, fixed cells were blocked and permeabilised with blocking buffer (5%
861 wt/vol bovine serum albumin (Sigma-Aldrich) and 0.5% vol/vol Triton X-100 in PBS) for 30
862 min and then incubated with 1 μ g/mL primary antibody against DNA polymerase I
863 (ab188424, Abcam) in blocking buffer for 60 min at room temperature. After washing with
864 PBS three times, the cells were incubated with 2 μ g/mL fluorescently labelled secondary
865 antibody (Alexa 647, A20006, ThermoFisher) against the primary antibody in the blocking
866 buffer for 40 min at room temperature. After washing with PBS three times, the cells were
867 postfixed with 4% (wt/vol) paraformaldehyde in PBS for 10 min and stored in PBS before
868 imaging. STORM image analysis, drift correction, image rendering, protein cluster
869 identification and images presentation were performed using Insight342, custom-written
870 Matlab (2012a, MathWorks) codes, SR-Tesseler (IINS, Interdisciplinary Institute for
871 Neuroscience) (72), and Image J (National Institutes of Health).

872

873 **Statistical analysis**

874 Statistical analysis was performed using GraphPad Prism v.9.0.0. All data are presented as
875 individual values and mean or mean \pm SEM. Unless otherwise specified, statistical
876 comparisons were conducted using one-way ANOVA (for multiple groups) or unpaired two-
877 tailed Student's t-tests (for two-group comparisons), assuming a 95% confidence interval. A
878 probability value of $P < 0.05$ was considered significant. Statistical significance is indicated
879 in each figure. All remaining experiments were repeated independently, at least six with
880 similar results.

881

882 **Data availability**

883 Sequence data supporting this study's findings have been deposited in the GEO repository
884 with the GEO accession number GSE179434.

885

886 **Figure 1-figure supplement 1. Long-term exposures to ampicillin induced the evolution**

887 **of resistance in the wild type and $\Delta recA$ *E. coli* strain. (A)** The experimental flow of ALE

888 antibiotic treatment experiment. An overnight culture (0.6 mL; 1×10^9 CFU/mL cells) was

889 diluted 1:50 into 30 mL LB medium supplemented with 50 $\mu\text{g}/\text{mL}$ ampicillin and incubated

890 at 37°C with shaking at 250 rpm for 4.5 hours. After treatment, the antibiotic-containing

891 medium was removed by washing twice (20 min centrifugation at 1500 g) in fresh LB

892 medium. The surviving isolates were resuspended in 30 mL LB medium and grown overnight

893 at 37°C with shaking at 250 rpm. Ampicillin treatment was applied to the regrown culture and

894 repeated until resistance was established. **(B)** Changes in the MICs of ampicillin in the wild

895 type and $\Delta recA$ strain after 21 days of treatment with ampicillin at 50 $\mu\text{g}/\text{ml}$ for 4.5 hours

896 each day. MICs were measured after each daily treatment. Each experiment was

897 independently repeated at least twice, and the data are shown as mean \pm SEM.

898

899 **Figure 1-figure supplement 2.** The survival rate after a single exposure to ampicillin at 50

900 $\mu\text{g}/\text{ml}$ for 0,2,4,6, and 8 hours in the wild type and $\Delta recA$ strain.

901

902 **Figure 1-figure supplement 3. Single exposures to ampicillin induced the evolution of**

903 **resistance in the $\Delta recA^{CGSC}$ strain (JW2669-1).** (A) MICs of ampicillin were measured

904 against the wild type^{CGSC} *E. coli* strain after single exposures to ampicillin. **(B)** MICs of

905 ampicillin were measured against the $\Delta recA^{CGSC}$ strain after single exposures to ampicillin.

906 Each experiment was independently repeated at least six times using parallel replicates, and

907 the data are shown as mean \pm SEM. Significant differences among different treatment

908 groups are analyzed by independent t-test, * $P < 0.05$, ** $P < 0.01$, *** $P < 0.001$.

909

910 **Figure 1-figure supplement 4. Single exposures to other β -lactam antibiotics induced the**

911 **evolution of resistance in the $\Delta recA$ strain. (A)** MICs of penicillin G in the wild type,

912 $\Delta recA$, and complemented $\Delta recA$ strain, where the expression of RecA was restored, after

913 single exposures to penicillin G at 1 mg/mL for 8 hours. **(B)** MICs of carbenicillin in the wild

914 type, $\Delta recA$, and complemented $\Delta recA$ strain, where the expression of RecA was restored,

915 after single exposures to carbenicillin at 200 $\mu\text{g}/\text{mL}$ for 8 hours. Each experiment was

916 independently repeated at least six, and the data are shown as mean \pm SEM.

917

918 **Figure 1-figure supplement 5. Distribution fitting and fluctuation analysis support a**
919 **selection-driven resistance mechanism in the *ΔrecA* strain. (A)** Rifampicin-resistant
920 mutant counts from replicate cultures were fitted to theoretical Poisson distributions based on
921 observed means. **(B)** Fluctuation analysis using the Luria-Delbrück framework revealed long-
922 tailed, highly skewed mutation count distributions in the *ΔrecA* strain under the treatment of
923 ampicillin, characteristic of jackpot cultures arising from early-arising resistant mutants.

924

925 **Figure 2-figure supplement 1. The activity of β -lactamase was increased in the *ΔrecA***
926 **culture supernatants.** The *ΔrecA* strain was treated with ampicillin at 50 μ g/ml for 8 hours,
927 and surviving isolates harbouring the *ampC* mutations were selected. The level of β -
928 lactamase in cell culture supernatants was determined by the absorbance at OD₄₉₀. The levels
929 of β -lactamase in the wild type or *ΔrecA* strain culture supernatants without exposure to
930 ampicillin were tested as a control. Each experiment was independently repeated six times.
931 Each experiment was independently repeated at least six, and the data are shown as mean \pm
932 SEM.

933

934 **Figure 4-figure supplement 1. Transcriptional responses of the wild type and *ΔrecA***
935 **strain after single treatments with ampicillin for 8 hours.** GO analysis was performed
936 following the GOseq approach, and different genes in the wild type **(A, left)** and the *ΔrecA*
937 strain **(B, left)** were plotted. KEGG pathway enrichment was assigned according to the
938 KEGG database, and different genes in the wild type **(C, left)** and the *ΔrecA* strain **(D, left)**
939 were plotted. The top 20 enrichment pathways are listed in the GO and KEGG enrichment
940 analysis **(A-D, right).** Total RNA-seq was performed with three repeats in each group.

941

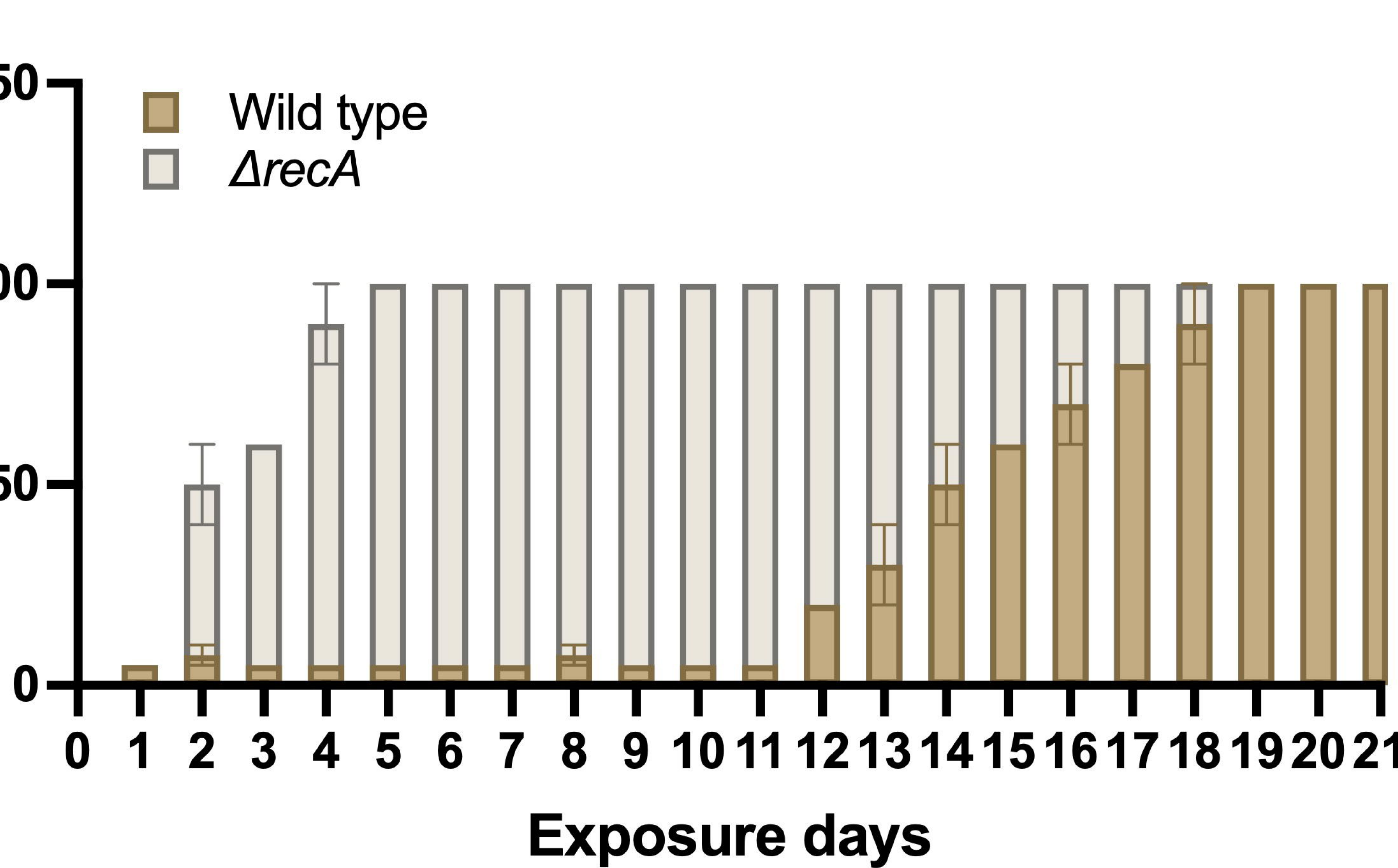
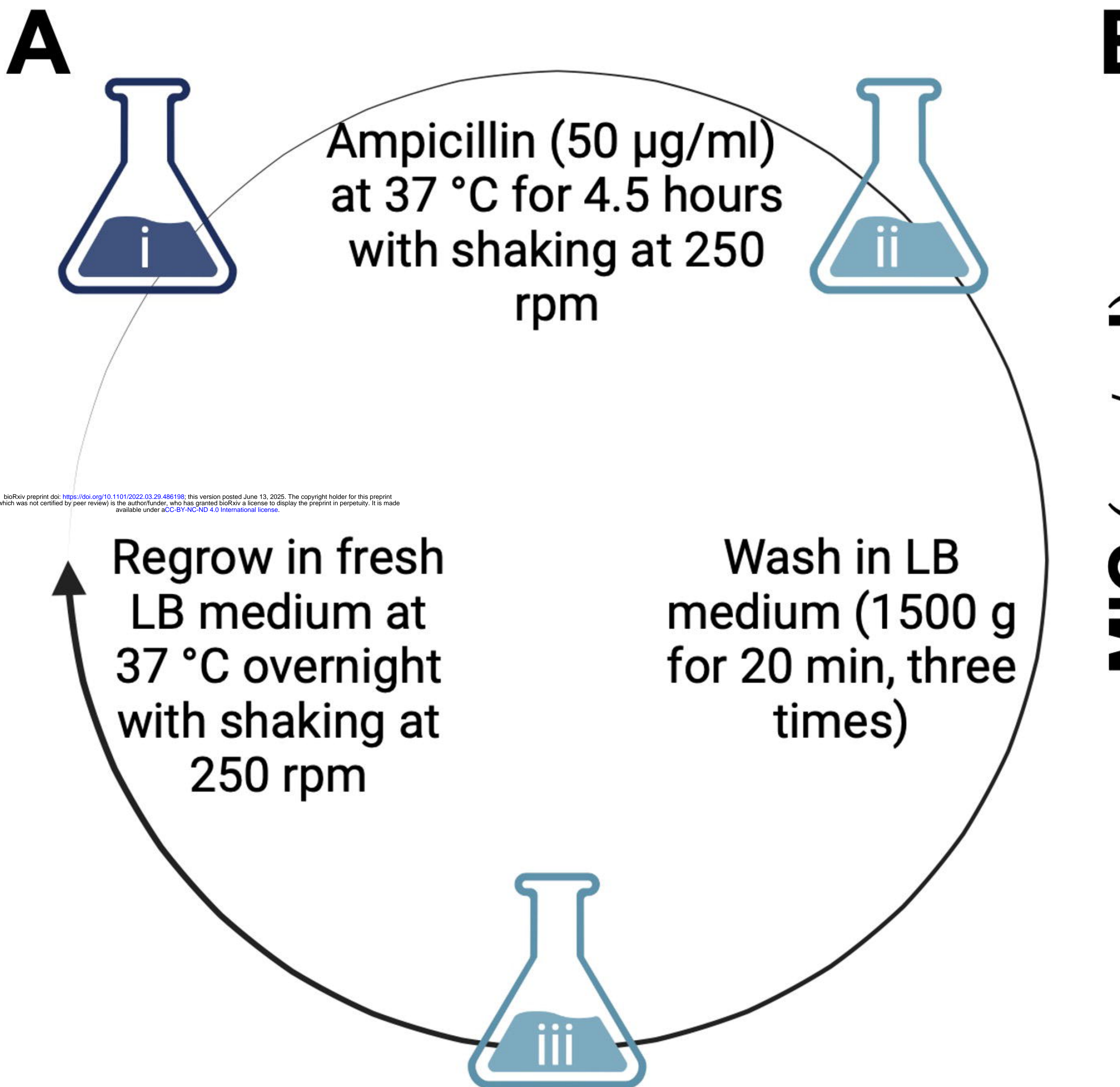
942 **Supplementary File 1. Table S1. Other mutations detected in the *ΔrecA* resistant isolates**

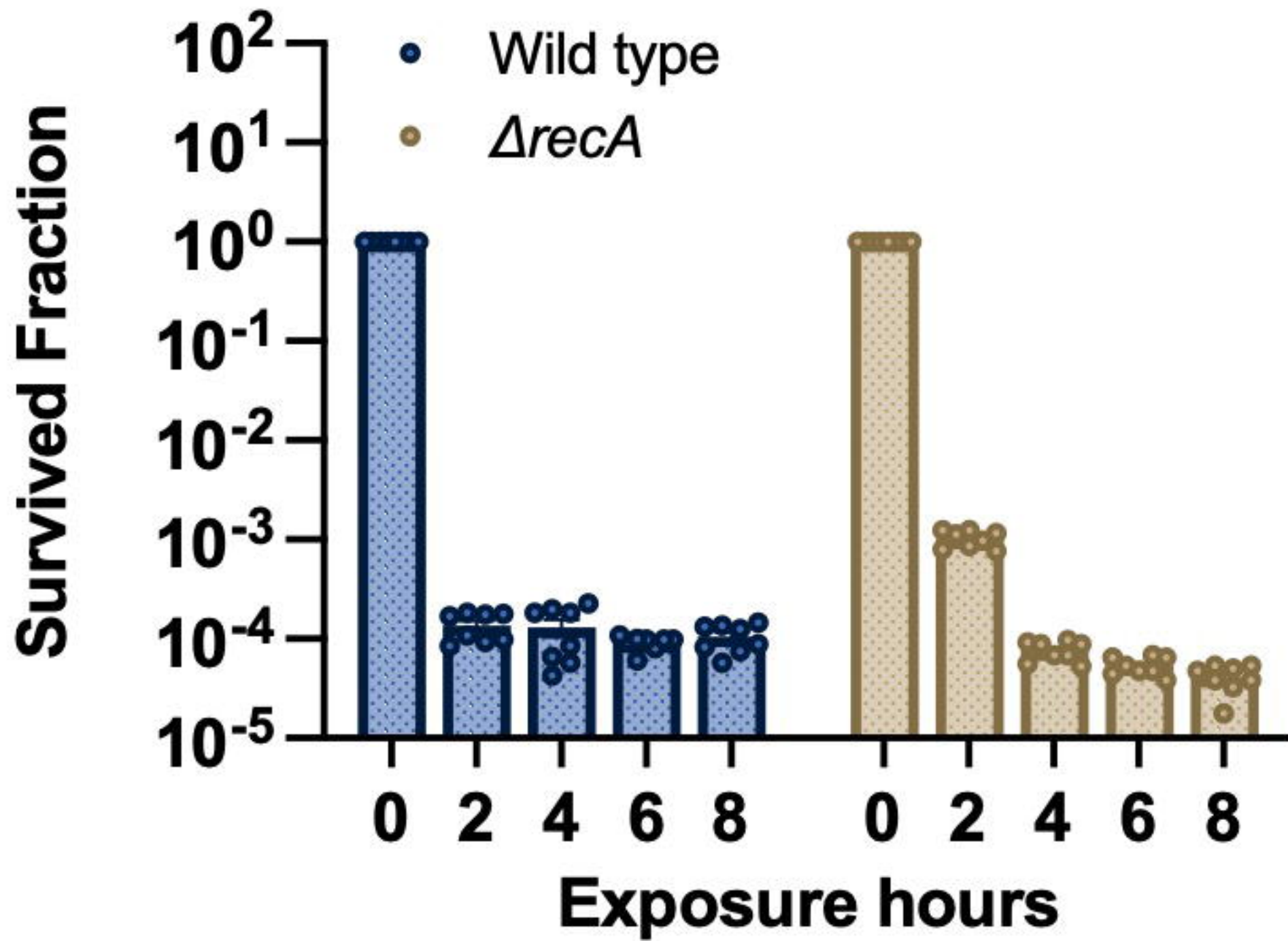
943 **Supplementary File 2. Table S2. Strains used in this study**

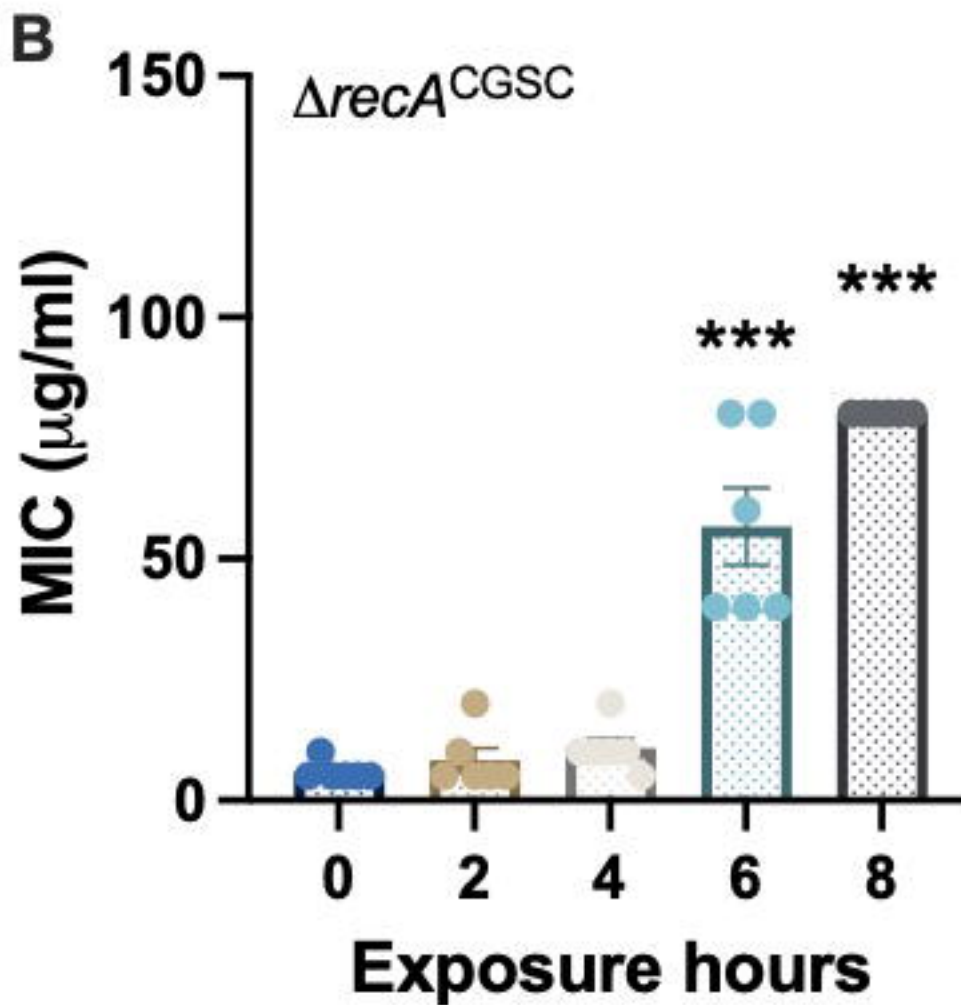
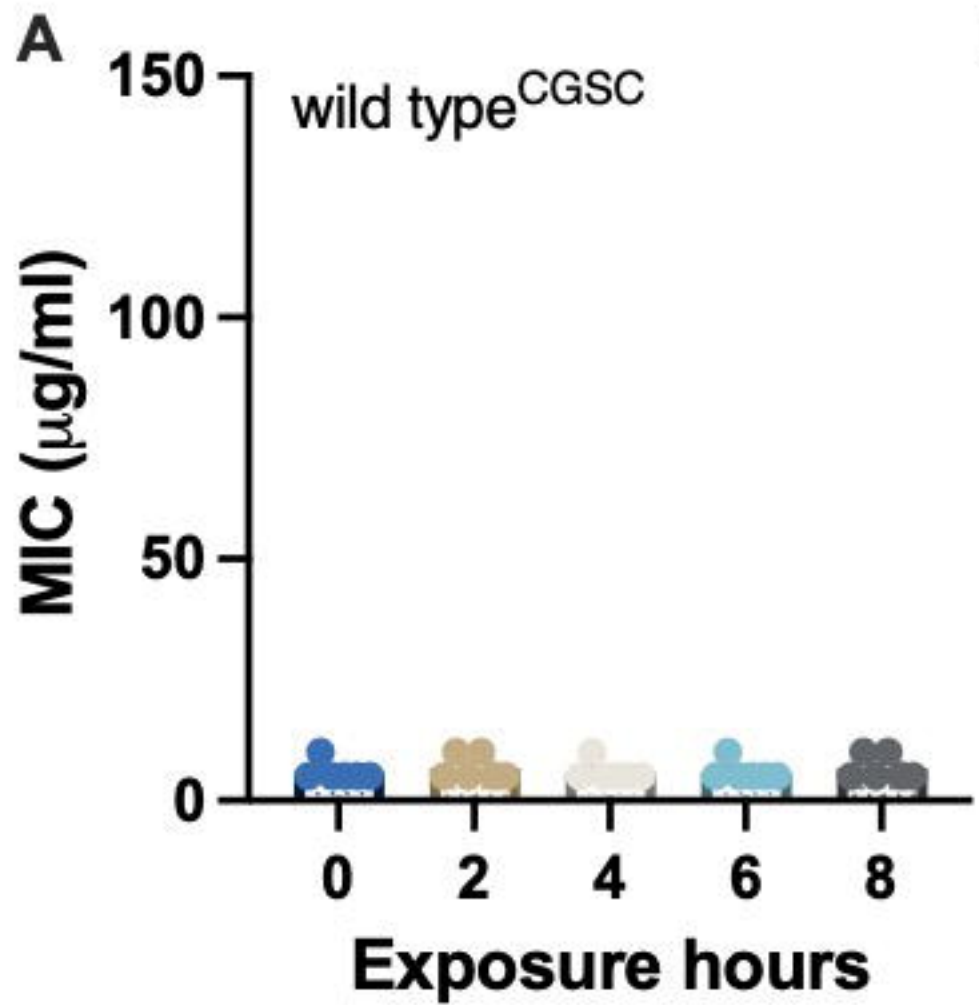
944 **Supplementary File 3. Table S3. Plasmids used in this study**

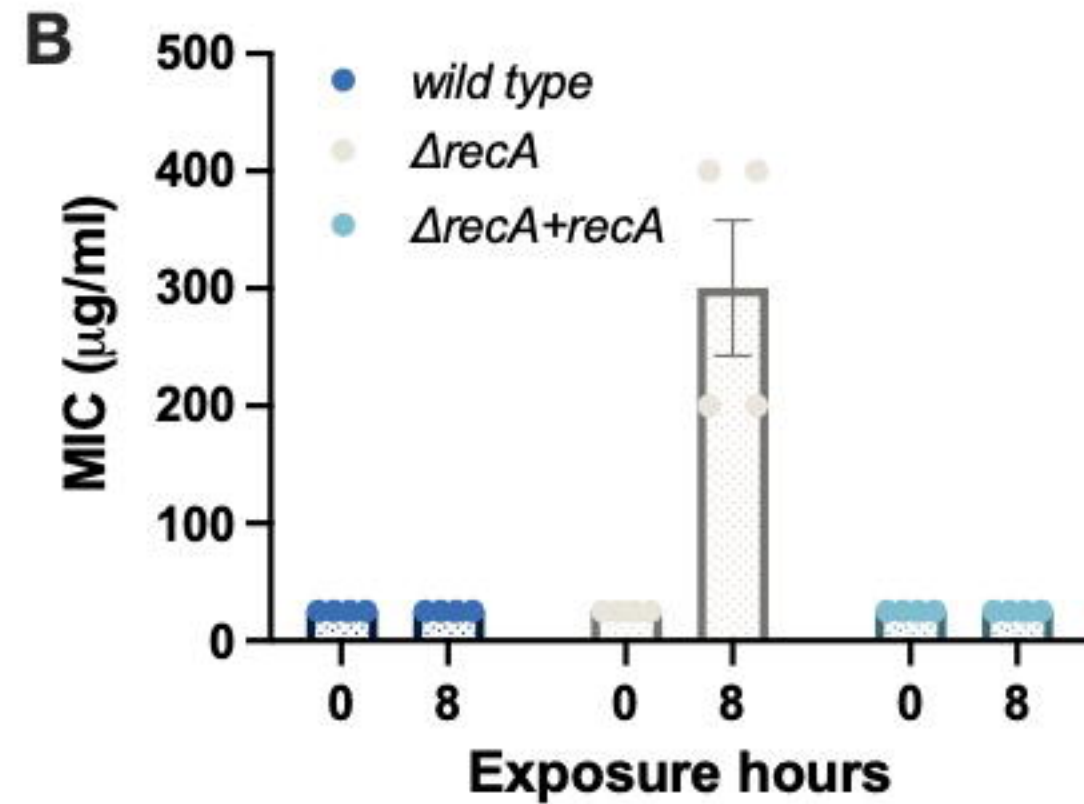
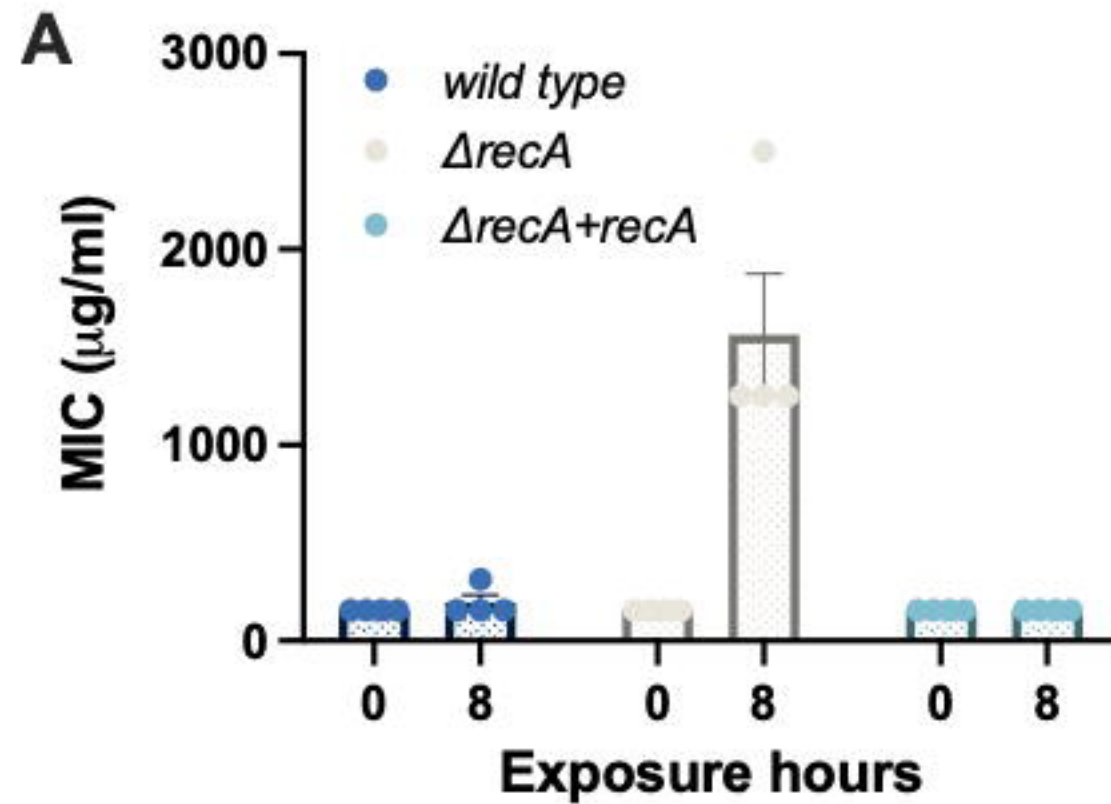
945 **Supplementary File 4. Table S4. Primers used in this study**

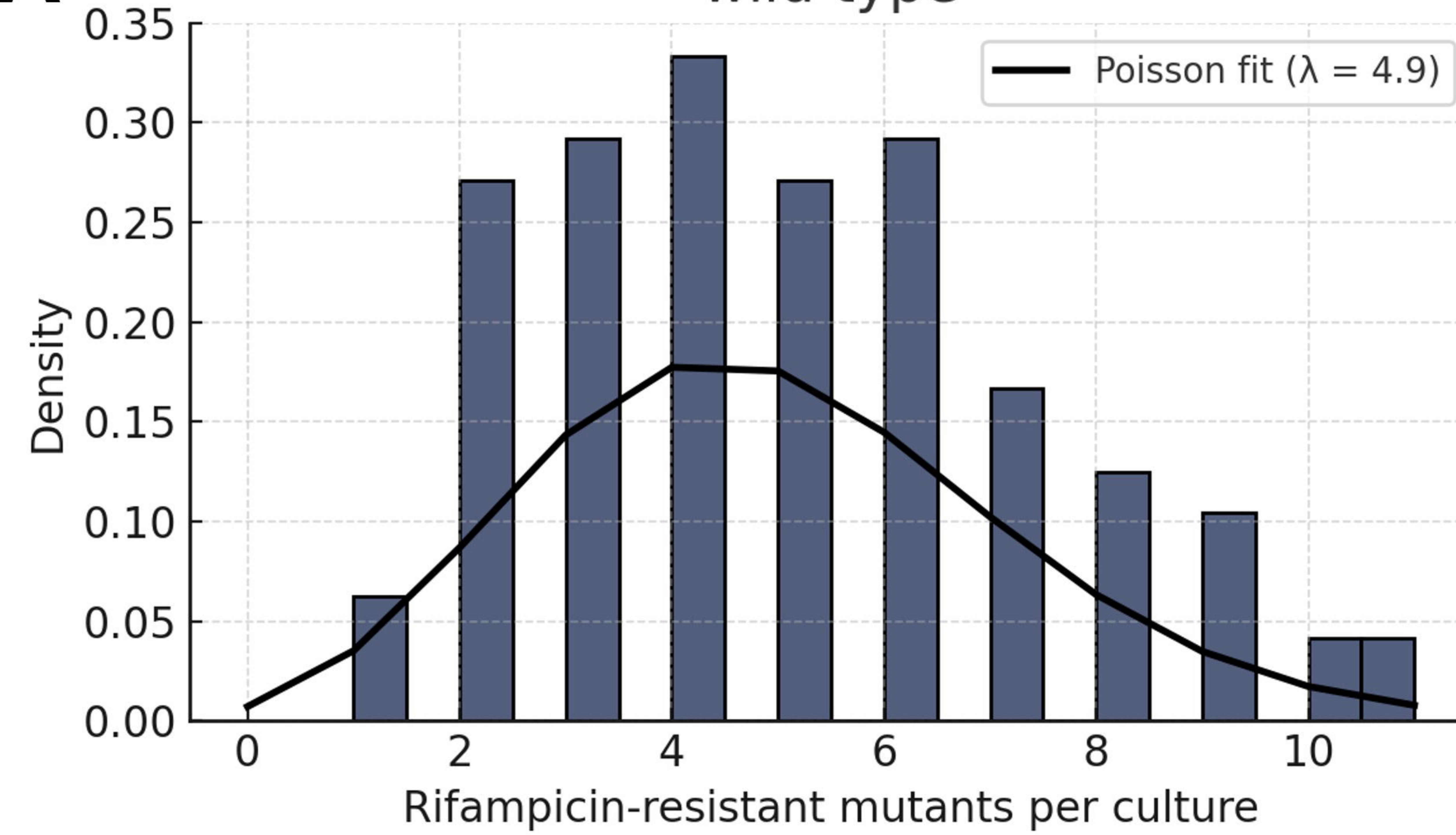
946



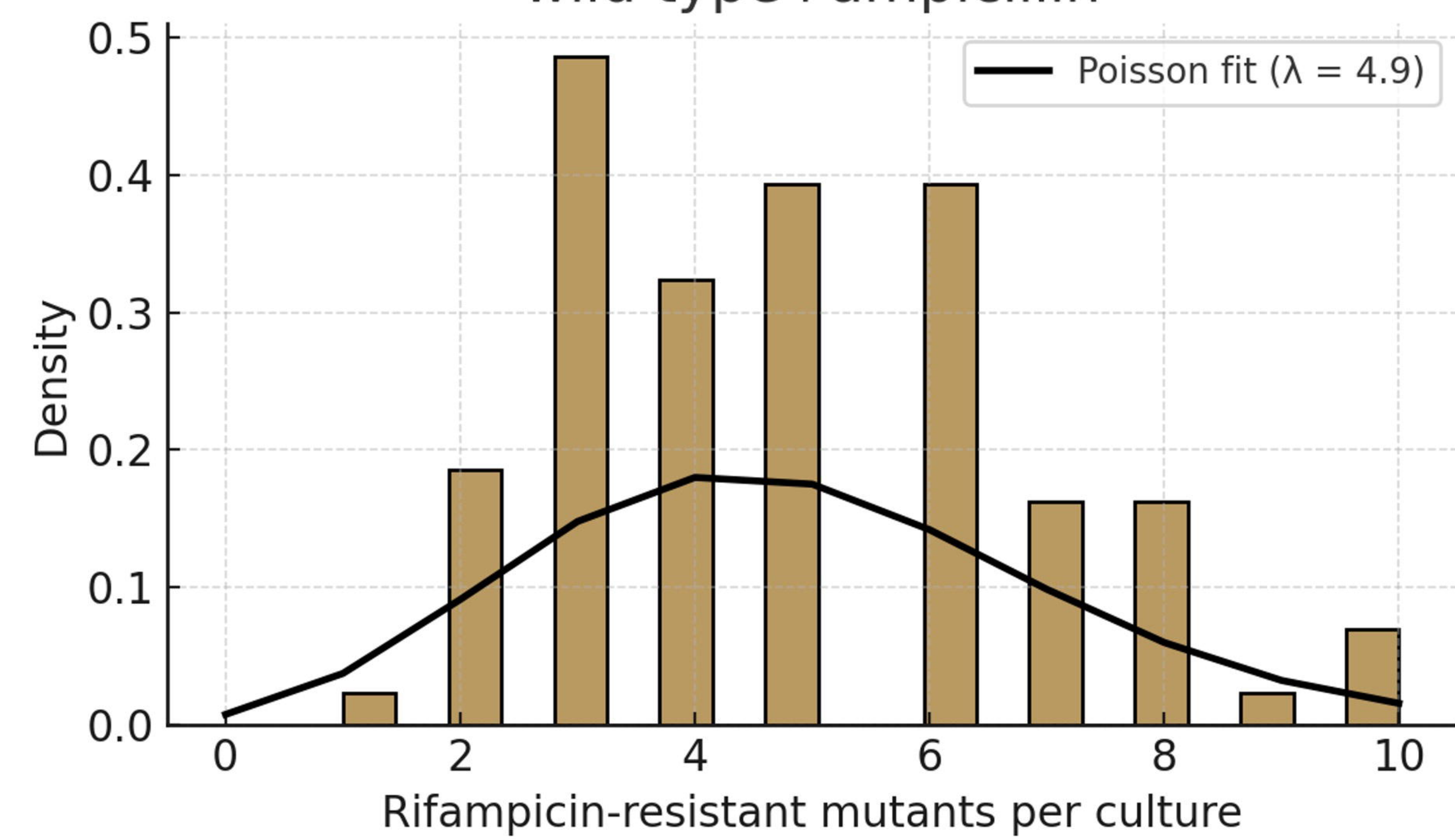
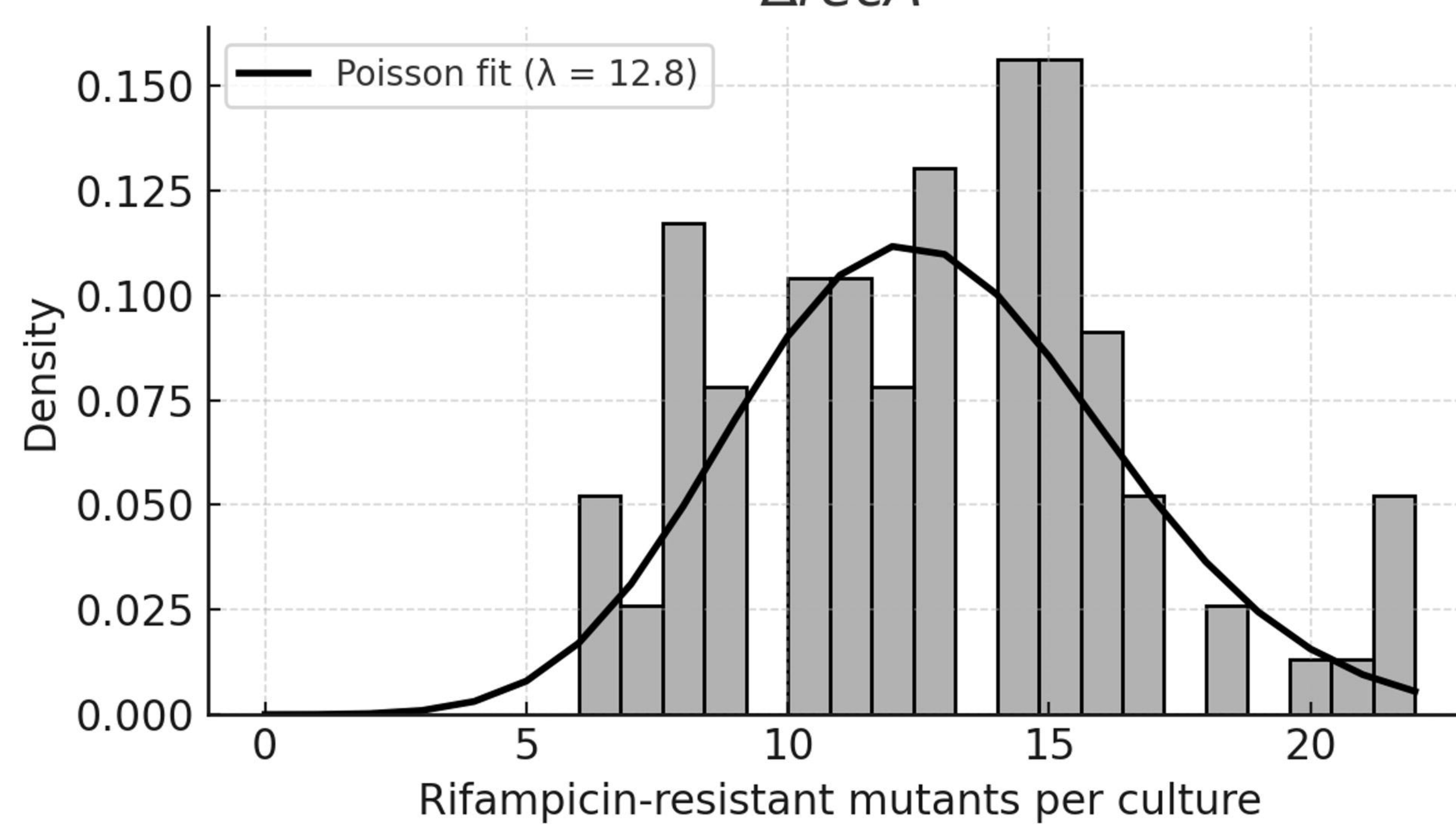
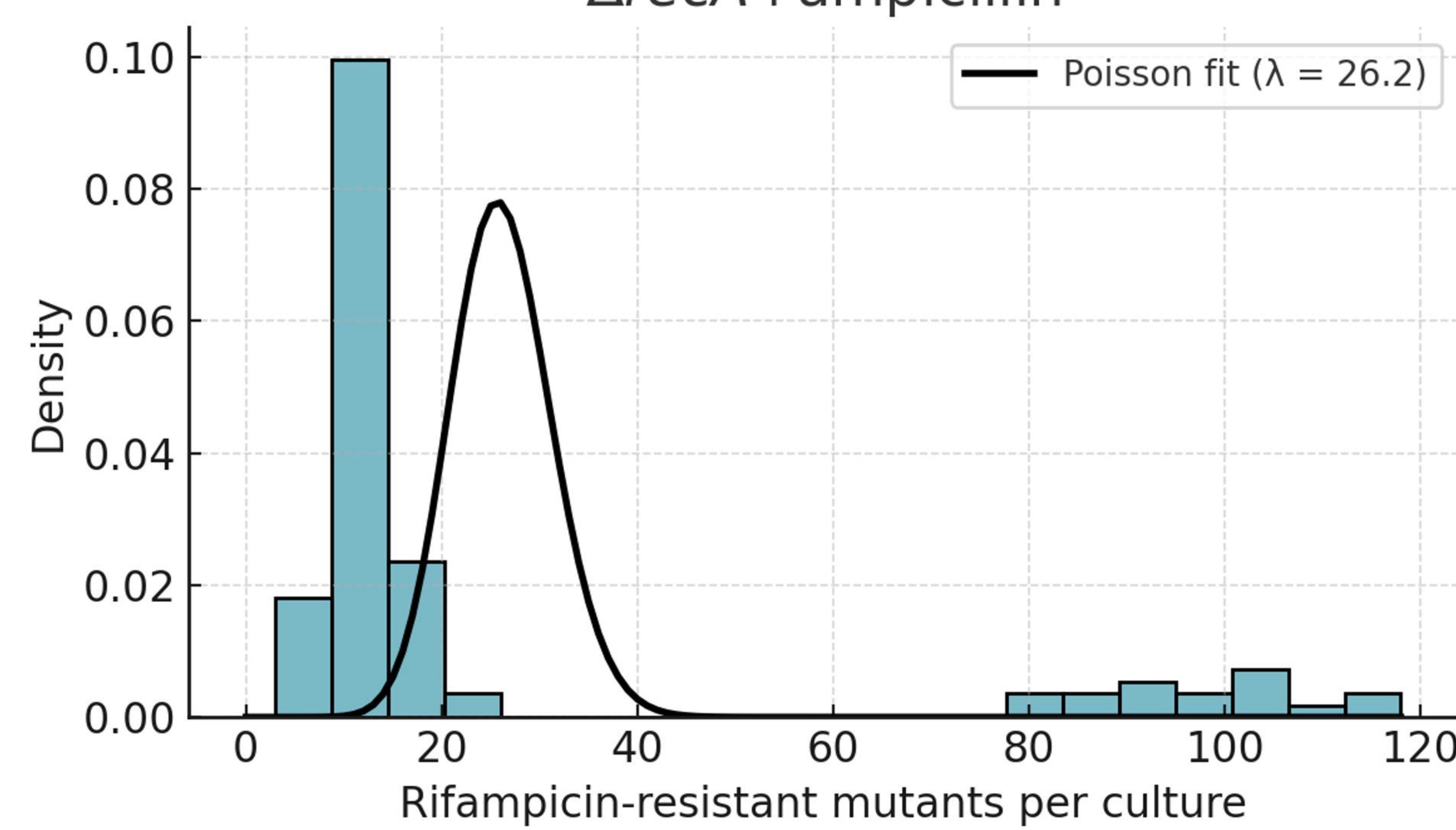
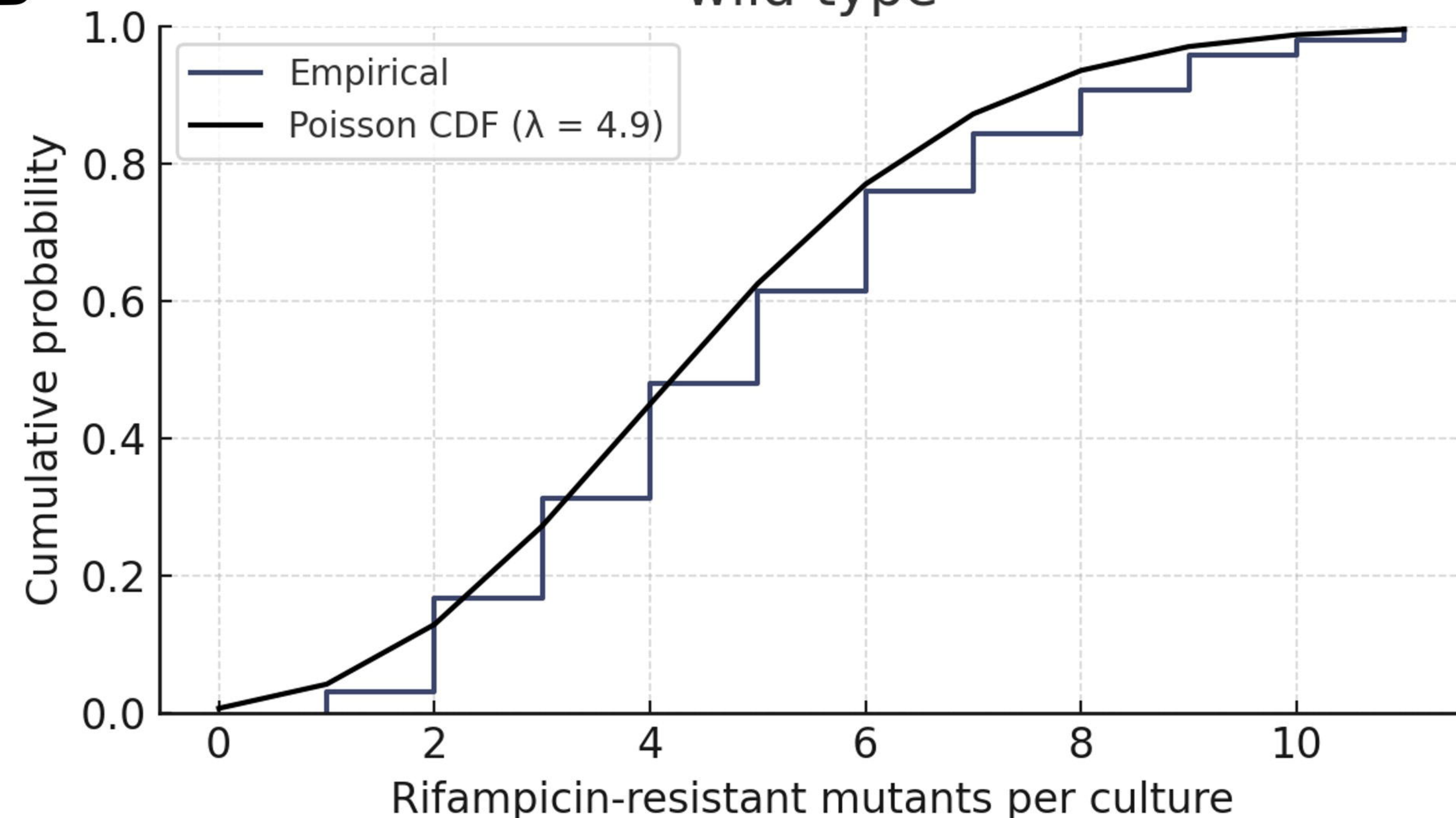




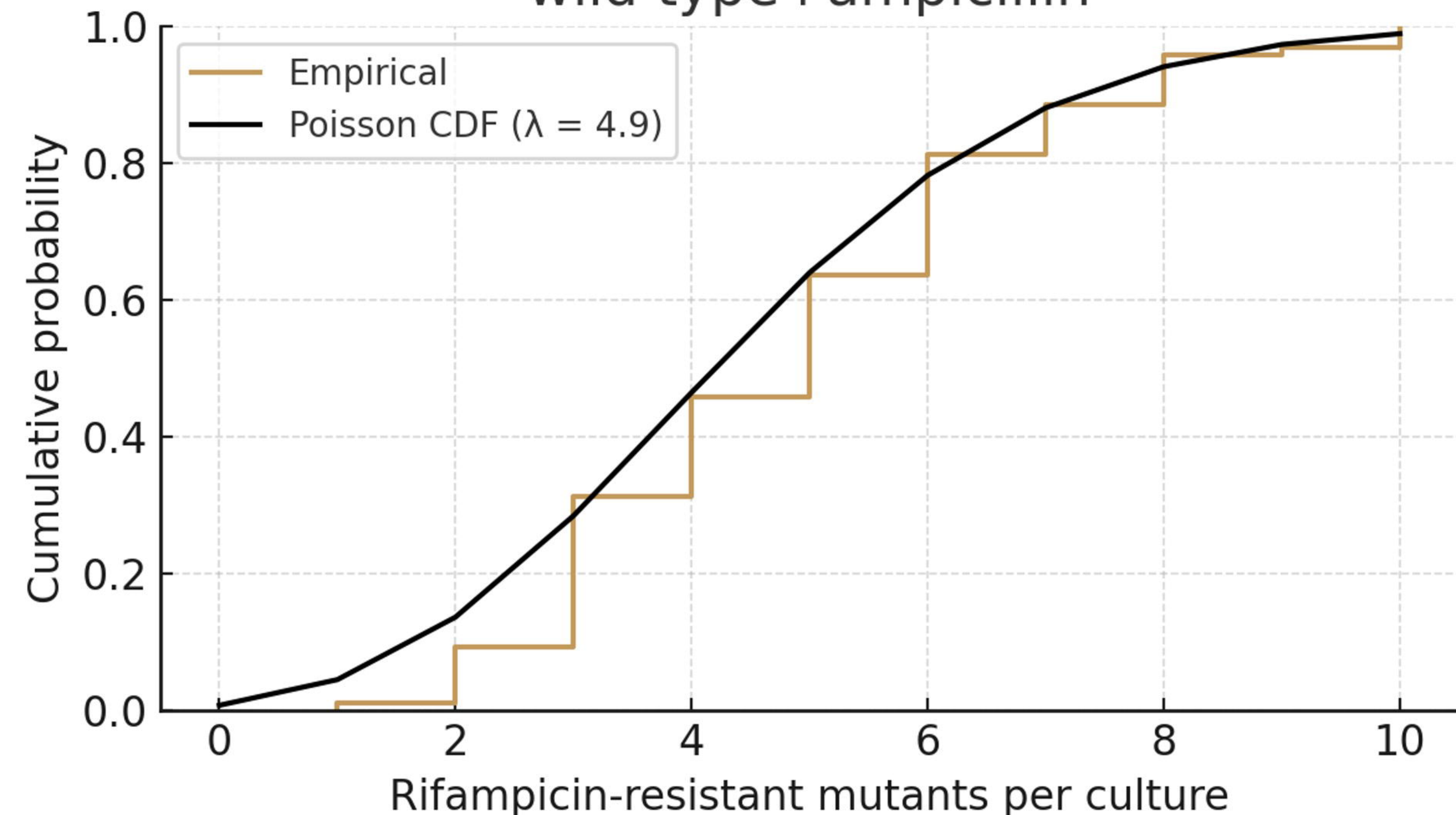
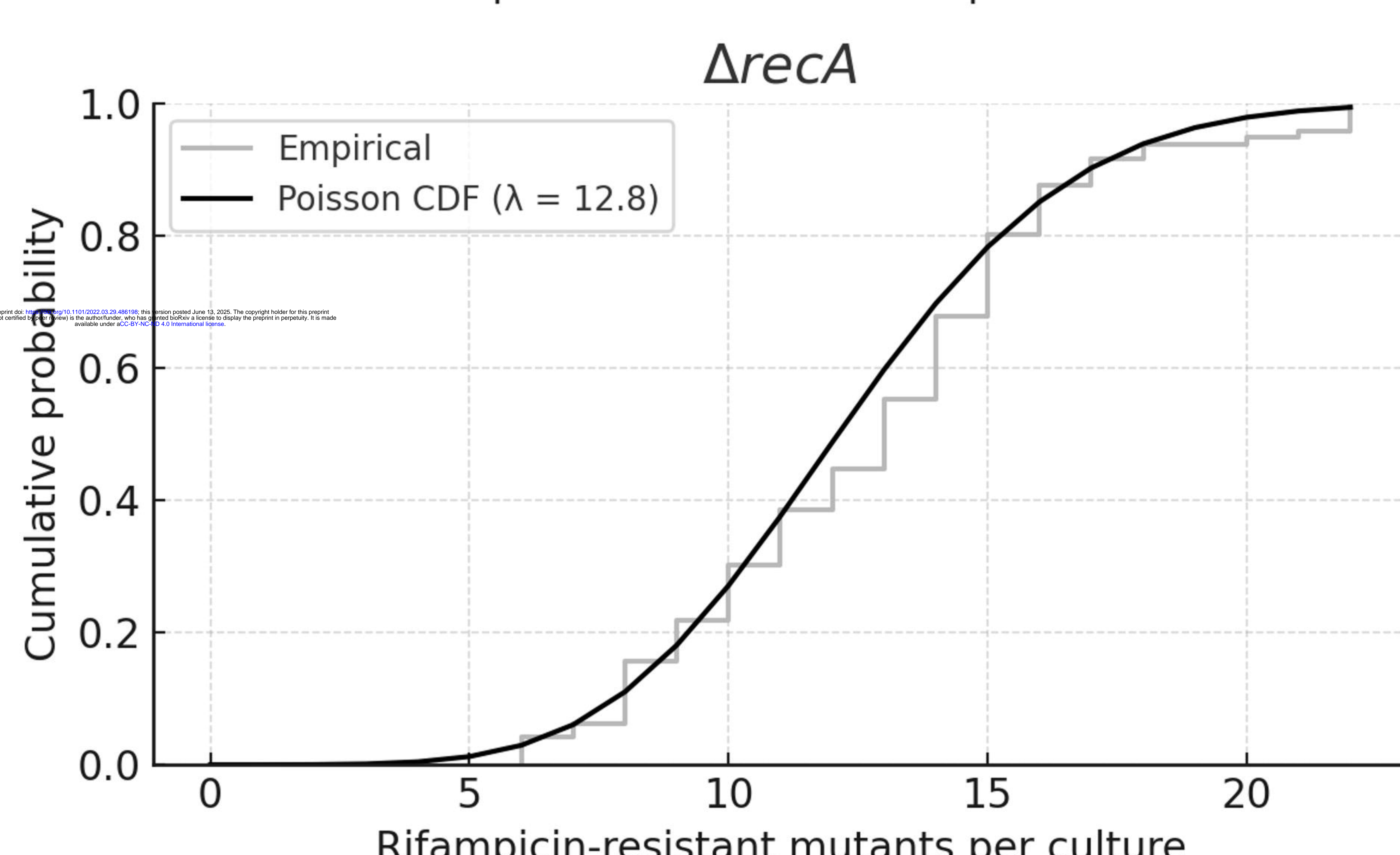


A wild type

wild type+ampicillin

 $\Delta recA$  $\Delta recA+ampicillin$ **B** wild type

wild type+ampicillin

 $\Delta recA$  $\Delta recA+ampicillin$ 